TRITIUM DIFFUSION IN NONMETALLIC SOLIDS OF INTEREST FOR FUSION REACTORS

CONTRIBUTORS:

C. Alexander
R. Causey
D. Chari
T. Elleman (Principal Investigator)
P. Feng
J. Fowler
H. Palmour
A. Payne
D. Rao
C. Ravanbakht
R. Roberts
K. Verghese
L. Zumwalt

Department of Nuclear Engineering
North Carolina State University
Raleigh, North Carolina 27650

FINAL REPORT

Contract No. DE-AS05-76ET52022

DISCLAIMER

TRITIUM DIFFUSION IN NONMETALLIC SOLIDS OF INTEREST FOR FUSION REACTORS

CONTRIBUTORS:

C. Alexander
R. Causey
D. Chari
T. Elleman (Principal Investigator)
P. Feng
J. Fowler
H. Palmour
A. Payne
D. Rao
C. Ravanbakht
R. Roberts
K. Verghese
L. Zumwalt

Department of Nuclear Engineering
North Carolina State University
Raleigh, North Carolina 27650

FINAL REPORT

Contract No. DE-AS05-76ET52022

ABSTRACT

Tritium diffusion measurements have been conducted in Al_2O_3, BeO, Y_2O_3, SiC, B_4C, Si_3N_4 and pyrolytic carbon as a basis for evaluating these materials as potential tritium barriers in fusion reactors. Deuterium solubility measurements were conducted with Al_2O_3, SiC and pyrolytic carbon to establish the pressure and temperature dependence of solubility and to identify solubility ranges. Hydrogen permeability measurements on commercially available Al_2O_3 and SiC materials were used as a check on calculated permeabilities and to provide data on hydrogen permeation rates in polycrystalline materials. The diffusion, solubility and permeation results are presented and discussed in terms of fusion reactor applications.

TABLE OF CONTENTS

LIST OF FIGURES

LIST OF TABLES

INTRODUCTION

The diffusion of tritium in fusion reactors is likely to be important in controlling the inventory and distribution of tritium within the blanket and in the proper operation of the reactor. For example:

- Diffusion of tritium injected into the first wall from the plasma can lead to loss of tritium from the plasma and tritium buildup in the blanket. The tritium can then be redistributed by diffusion to other blanket components.

- The circulation of coolant through a heat exchanger provides a route whereby tritium in the coolant can diffuse through heat exchanger walls and subsequently be released to the environment.

- The potential success of solid breeder blankets may largely be determined by the ease with which tritium can be readily recovered from the materials by diffusion for repurification and injection into plasma.

- Tritium permeation through permeable membranes has been considered as a continuous purification scheme for recovering tritium bred in the blanket and is a process dependent upon proper control of diffusion parameters.

A wide variety of possible fusion reactor blanket designs are now evolving, but all of them involve some understanding of tritium transport rates through blanket components and tritium solubilities in contacted materials.

Considerable data exist on hydrogen permeation, dissolution and diffusion in metals but far less work has been reported for metal oxides, nitrides, carbides and other potential nonmetallic reactor construction and insulator components. It is now recognized that ceramics will be utilized in fusion reactor blankets. Low Z first wall coatings are needed to prevent plasma contamination, electrical insulators are required for neutral beam injectors and charge collectors, and the low activation properties of ceramics coupled with their high temperature strength makes their use attractive in some structural applications. The brittle nature of ceramics, sometimes cited as a disadvantage, is not necessarily so if this is accommodated by proper design. Furthermore, metals under fusion reactor irradiation conditions may become as brittle as some ceramics. It is, therefore, desirable to have data on hydrogen solubility and transport in nonmetallic solids as well as for metal alloys.

The purpose of the present study was to provide base data on hydrogen diffusion, solubility, and permeation of nonmetallic solids of potential interest for fusion applications. A secondary objective was to evaluate the potential of these materials as tritium diffusion barriers assuming that appropriate deposition techniques can be devised. The program has resulted in the measurement of diffusion coefficients for a number of ceramic materials of potential interest and the measurement of hydrogen solubilities and permeabilities in a smaller number of materials. Although tritium is the hydrogen isotope of interest, experimental limitations dictated the use of deuterium or normal hydrogen in specific applications. Results have been tabulated for the specific isotope employed and approximate corrections for tritium may be made by employing the inverse square root of mass corrections.

Most of the program results have been presented in the open literature and only a summary of results is presented here. Appendix A summarizes the publications resulting from this work to date. A detailed review of the literature related to hydrogen diffusivity, solubility and permeability of nonmetallic solids has been prepared under this program and will be released as a DOE report.

EXPERIMENTAL TECHNIQUES

I. Diffusion Studies

A. Recoil Injection. Most tritium diffusion measurements were conducted by surrounding specimens with 96% enriched ^{6}LiF or $^{6}Li_2CO_3$, irradiating with the NCSU PULSTAR Reactor to inject transmutation produced tritium, and subsequently measuring the time rate of tritium release to establish diffusion coefficients. The enriched lithium carbonate or lithium fluoride was purchased as powder through ORNL. The powder was distributed on a defined region of the specimen surface to yield a layer approximately 16mg cm^{-2} which is effectively infinitely thick for the recoil tritons. The powder was held in place during irradiation with tape and through the use of a specimen capsule that stacked specimens against each other. A typical reactor irradiation was for 2 hours at 50 kilowatts ($2x10^{14} ncm^{-2}$) which yielded a maximum surface tritium concentration of about 0.1 ppm (by weight). Higher reactor power produced specimen heating and led to premature release of the tritium. Specimens were dried prior to irradiation to remove absorbed water and stored in desiccators prior to heating. Powdered specimens were either separated from the lithium salt by thin (0.1 mil) mylar films or else were mixed with the lithium salt and separated subsequent to irradiation. Separation was accomplished by dissolving the lithium salt or slurrying mixed powders to separate the denser specimen powders.

Tritium released from specimens during postirradiation heating was measured by passing a sweep gas over the specimens and through a proportional counter or ion chamber. Count-rate or ionization current was continuously recorded for later plotting and data analysis. Figure 1 presents a schematic diagram of the tritium release apparatus. At the conclusion of a release experiment, the specimens were heated to elevated temperatures to remove all tritium and obtain a total quantity for the calculation of a release fraction. Diffusion coefficients were calculated from the expression[1]

$$f(t) = \frac{4}{R}\sqrt{\frac{Dt}{\pi}} \quad f(t)<0.3 \qquad (1)$$

R = recoil range (cm)

D = diffusion coefficient ($cm^2 sec^{-1}$)

t = heating time (sec)

The recoil injection method was typically useful in the determination of diffusion coefficients lying within the range $1x10^{-16}cm^2sec^{-1}$ to $1x10^{-9}cm^2sec^{-1}$. Higher values of D produced gas release so rapid that the kinetics could not be resolved while lower D's produced unacceptably long run times and low counting rates. Sample temperatures were, therefore, selected to encompass the indicated range of diffusion coefficients and different temperatures were employed for different specimens. Tritium release kinetics were generally consistent with equation (1) and plots of the determined diffusion coefficients yielded single-valued diffusion activation energies.

B. Release of Dissolved Deuterium. The deuterium solubility studies yielded plots of deuterium release versus time and temperature. The deuterium was introduced through high temperature dissolution as described in Section II. The kinetics of release at constant temperature could be measured with a mass spectrometer and provided a useful check on diffusion coefficients measured through recoil injection. Diffusion coefficients determined from the release of dissolved deuterium were obtained for several of the materials studied.

C. Diffusion Kinetics in Permeation Studies. The permeation experiments provided a measure of hydrogen transport through sintered specimens of alumina and silicon carbide. The experimental system used in permeation studies is described in Section III. Sudden changes in temperature or pressure produced a change in permeation rate that reached equilibrium at a rate determined by the specimen diffusion coefficient. The kinetic data taken during temperature or pressure transients could, therefore, be used to obtain diffusion coefficients in permeation specimens. The equation employed is given by

$$\left.\begin{aligned} &\frac{\partial C}{\partial t} = D\left(\frac{\partial^2 C}{\partial r^2} + \frac{1}{r}\frac{\partial C}{\partial r}\right) \quad a \le r \le b \\ &C(r,0) = C_o \ln (b/r)/\ln (b/a) \\ &C(a,t) = C_1 \\ &C(b,t) = 0 \\ &R(t) = \frac{2\pi C_1 D}{\ln(b/a)} + 4\pi D(C_1 - C_o)\sum_{r=1}^{\infty} \frac{J_o(a\alpha_n)J_o(b\alpha_n)e^{-D\alpha_n^2 t}}{J_o^2(a\alpha_n) - J_o^2(b\alpha_n)} \end{aligned}\right] \quad (2)$$

where α_n are the roots of $J_o(\alpha_n a)Y_o(\alpha_n b) - J_o(\alpha_n b)Y_o(\alpha_n a) = 0$

The measurement of permeation rate is described in a later section.

II. Solubility Studies

A. Deuterium Dissolution. Hydrogen solubility measurements were made on aluminum oxide, silicon carbide and pyrolytic carbon. Powdered specimens were exposed to known deuterium atmospheres at elevated temperatures for time periods four to six times those calculated for dissolution equilibrium of hydrogen. The mean-square transport for a diffusing species is given by:

$$\overline{x^2} = 6Dt \qquad (3)$$

Specimen equilibration with a dissolved gas should be approximately complete for values of $\overline{x^2}$ equal to or larger than the particle radius. The diffusion coefficients determined in earlier work were used to establish these equilibration times. It was assumed that no kinetic barriers for deuterium dissolution existed at the powdered surfaces and the presence of barriers is a potential source of error that could lead to low apparent values for solubility.

Powdered specimens equilibrated with deuterium were heated isochronally in a vacuum furnace to temperatures ranging to 1200°C. A UTI model 100C quadruple mass spectrometer was used to monitor the composition of the released gas. A schematic drawing of the solubility apparatus and a photograph are included in Figures 2 and 3. Deuterium released as gas (HD, D_2) or as water vapor (HDO, D_2O) were monitored. No other chemical forms of released deuterium were detected, although other workers[2,3] have observed extremely small fractions of injected hydrogen appearing as hydrocarbons in a release stream.

The mass spectrometer was calibrated for gaseous hydrogen by decomposing known quantities of titanium deuteride (TiD_2) and correlating the peak height with the known deuterium concentration. Calibrations for water vapor were effected by oxidizing the deuterium from known titanium deuteride concentrations to D_2O and measuring the deuterated water peaks.

Some releases of deuterium as deuterated water at low temperatures were occasionally observed in aluminum oxide and were attributed to release of absorbed water vapor. These contributions were not included in the solubility

calculations. The total deuterium released up to 1200°C. was assumed to comprise the total dissolved deuterium and was used as the basis for calculation of the solubility values. Higher temperatures were not employed as deuterium release dropped to negligible values by 1200°C. The deuterium in water vapor that appeared at elevated temperatures was assumed to result from surface or post-release exchange and was included in the solubility calculations for deuterium.

B. Hydrogen Solubility From Permeation Specimens. The alumina and silicon carbide tubes used in the permeation studies contained dissolved hydrogen and tritium at the conclusion of a permeation run. The tritium gas on the inside of the tube was replaced with an inert sweep gas and the tubes were then heated to remove dissolved hydrogen with a collection sweep gas passing over the inner and outer specimen surfaces. The released tritium was detected as a measure of the gas dissolved in the tube. These data were also used to calculate hydrogen concentrations produced by dissolution and the results are included in discussions on solubility. Specimen temperature was not uniform over the entire length of the heated regions and an iterative technique was employed to correct solubilities for the non-uniform temperature distributions.

III. Permeation Studies

Hydrogen permeation studies were conducted on silicon carbide and alumina tubes to provide information on the permeabilities of commercially available materials and as a check on the diffusivity and solubility values. The permeation apparatus consisted of a large reservoir to store a hydrogen/helium/tritium gas mixture and a bellows pump that circulated the gas through a heated ceramic tube. Figure 4 presents a schematic of the permeation apparatus. A helium flow gas was passed over the external surface of the heated ceramic tube to collect permeated tritium. This gas was passed through an ion chamber for tritium detection. It was determined that the tritium absorbed in undesirably high fractions upon the system walls without the hydrogen flow gas and even with hydrogen, tritium absorption proved a problem. Background ionization currents increased steadily as a consequence of tritium absorption and it was necessary to clean the chamber at periodic intervals. The high tritium absorption rates seemed greater than would be expected from an assumption of complete isotopic exchange with the sweep gas, so there is a suspicion that

some tritium permeated the cermic tube as water vapor and did not completely exchange with the flow gas prior to transport to the system.

A grab sampler attached to the permeation apparatus was used to remove samples for tritium assay. This was accomplished by sweeping the grab sampler contents through the ionization chamber and recording the time dependent current signal. The permeation system was designed to operate at total pressures near atmospheric or slightly above and even though the principal system gas was helium, the hydrogen partial pressures were well above the low values that would be encountered in a fusion reactor. Permeation measurements were typically made over a hydrogen partial pressure range of 2 to 60kPa and a temperature range of 1000 to 1400^{o}C. The tritium tracer was injected by heating an irradiated lithium-6 salt, heating aluminum foils into which tritium had been injected, or fracturing ampoules containing known concentration of tritium gas. The last technique proved to be the most satisfactory and was, therefore, employed in most runs.

A typical permeation run was started by pressurizing the system and circulating the gas for several days to establish the absence of leaks. The system was then evacuated several times and backfilled with helium to remove most of the oxygen. The hydrogen/helium mixture was then added at the desired partial pressures to give a total system pressure slightly above one atmosphere. A tritium ampoule was fractured on a side arm and the gas circulated to reach isotopic equilibrium. The ceramic tube was then brought to desired temperature and the gas flow in the annulus started to detect permeating tritium. A cold trap in the circulating loop could be used to trap water vapor if desired. Grab samples were taken during the run to maintain a mass balance with diffusing tritium and the system pressure was monitored to establish the absence of leaks. Once the permeation rate at a given temperature had been established, the temperature was either changed to obtain a new value or the gas was released into an evacuated chamber to add hydrogen or helium to change the relative partial pressures. It was common practice during the run to change sweep gas flow rates and note the change in tritium current as a basis for checking ionization chamber performance and background. A calibrated radiation source was also periodically placed in a reproducible position adjacent to the ion chamber to check chamber operation during the run.

MATERIALS

An effort was made to secure samples of high purity and known composition for the diffusion and solubility studies. Measurements were made with single-crystal materials where available for the diffusion studies. Specimens with known high impurity concentrations were also obtained to give an indication of impurity effects on diffusion. Surface area measurements were conducted on powder samples to determine particle sizes through Micromeritics Instrument Corp., Norcross, Ga. Table I summarized the sources and specimen characteristics of the materials employed in the diffusion and solubility studies.

TABLE I

MATERIALS USED IN DIFFUSION, SOLUBILITY AND PERMEATION STUDIES

Material	Form	Purity	Source
DIFFUSION STUDIES			
Al_2O_3	Single-crystal	>99.9%	Union Carbide Corp. Linde Division
Al_2O_3	Sintered (1-6μm)	<50ppm MgO	Fabricated in Materials Engineering NCSU
Al_2O_3	Lucalox	99.8% Al_2O_3 0.2% MgO Si(traces)	General Electric Co.
Al_2O_3	Powder mean particle diameter 0.2μm(1)	<50ppm MgO	Aluminum Co. of America
BeO	Single-crystal	>99.95%	Rockwell International
BeO	Sintered (9μm grain size)	0.2% Mg 0.32% Si	Brush Wellman, Inc.
BeO	Powder mean particle diameter 0.4μm(1)	50ppm Si 40ppm Al	Brush Wellman, Inc.
SiC	α-Single crystal	Al(50ppm)	Carborundum Co.
SiC	α-Single crystal	Al(0.6%)	Carborundum Co.
SiC	β-Single crystal	-	Materials Engineering NCSU
SiC	β-Vapor deposited	Possible Excess C	Texas Instruments
SiC	β-Vapor deposited	Possible Excess C	General Atomic Co.
SiC	α-Hot Pressed	Al(1%)	Norton Company
SiC	β-Sintered	B(∿0.4%)	General Electric Co.

Material	Form	Purity	Source
C	LTI Pyrolytic Carbon ρ=1.785 gcm^{-3}	-	General Atomic Co.
C	Laminar Pyrolytic carbon ρ=1.89 gcm^{-3}	-	General Atomic Co.
C	Si Doped Pyrolytic carbon	40 w/o Si	General Atomic Co.
SCB Glass	-	SiO_2-46.1% BaO-31.3% Al_2O_3-8.3% TiO_2-12.5% Cr_2O_3-1.0% Eu_2O_3-0.8%	Atomics International
Y_2O_3	Hot Pressed, Grain Size - 30μm	>99.99%	Ceradyne Corp.
Y_2O_3	Yttralox	Y_2O_3-89% ThO_2-10% Nd_2O_3-1%	General Electric Co.
B_4C	Hot Pressed	-	Hanford Engineering Development Lab.
Si_3N_4	Sintered	-	Norton Company
SOLUBILITY STUDIES			
Al_2O_3	Single-crystal	>99.9%	Union Carbide Corp. Linde Division
Al_2O_3	Powder -0.2μm	>99.93% Al_2O_3	Aluminum Company of America
Al_2O_3	Powder -4.0μm	>99.55% .05% SiO_2 .04% Fe_2O_3 .02% MgO	Aluminum Company of America
SiC	β-Vapor deposited	Possible Excess C	General Atomics
SiC	α-Hot Pressed	Al(1%)	Norton Company
C	Laminar pyrolytic carbon ρ=1.89 gcm^{-3}	-	General Atomic Co.

Material	Form	Purity	Source
PERMEABILITY STUDIES			
Al_2O_3	High density, high purity sintered spec. grav. 3.85 (McDanel-No. 998), Tubes	99.8% SiO_2-.07% MgO-.05% CaO -.03%	McDanel Refractory Porcelin Co.
SiC	KT SiC, hot pressed, tubes	~9% free Si	Carborundum Co.

EXPERIMENTAL RESULTS

I. Alumina (Al_2O_3)

Tritium diffusion studies utilizing the recoil injection method were conducted for single-crystal, sintered, powdered, and MgO-doped specimens of Al_2O_3(Lucalox). The tritium release results were consistent with classical diffusion solutions (equation 1) and gave single values of diffusion activation energies on an Arrhenius plot. Since alumina is one of the more thoroughly studied of the materials, a plot of typical release curves has been included for this material only (Figure 5). In general, all specimens studied gave release kinetics that were consistent with classical diffusion solutions. The diffusion results for Al_2O_3 have been summarized in Figure 6 and Table II. The results for single-crystal and sintered alumina specimens were in generally good agreement but lesser agreement was obtained with the powdered specimens and MgO-doped crystals. A single best-fit line is included in the Figure for the powdered, single-crystal and sintered specimen results. Significant percentages of the tritium released from powdered samples was in condensible form, presumably reflecting near surface exchange with absorbed water. Some difference in release results for powders could be obtained depending upon whether the condensible fraction was trapped or allowed to enter the detector along with gaseous tritium. Figure 7 illustrates results for alumina where condensibles were alternately trapped and not trapped. The slightly lowered diffusion coefficients for single-crystal alumina compared with sintered alumina likely reflects some rapid diffusion paths created by open porosity in the sintered specimens. Given the inherent uncertainties associated with comparing diffusion results for sintered, single-crystal and powdered specimens, the agreement in Figure 6 is regarded as acceptable.

The markedly higher diffusion results for MgO-doped alumina appear to reflect an impurity effect as the numbers are too high to be explained in terms of experimental error. Effects of impurities in the host lattice on atomic diffusion are well established in the literature[4,5] and there is evidence for enhanced diffusion of hydrogen in some systems. An additional indication of impurity processes has been observed in Section II with an aluminum-doped silicon carbide. A more detailed analysis of the tritium diffusion results in alumina and a comparison with other workers has been presented in a journal publication[6].

TABLE II. Measured tritium diffusion coefficients - least squares best-fit values for $D = D_0 \exp(-Q/RT)$ (D_0^+ is upper limit on D_0, D^- is lower limit on D_0, and $\sigma(Q)$ is the standard deviation of the activation energy.)

Material (S. C. = single crystal)	Number of Points	D_0 (cm^2/sec)	D_0^+ (cm^2/sec)	D_0^- (cm^2/sec)	Q (kcal/mole)	σ (Q) (kcal/mole)	Temperature Range (°C.)
Al_2O_3 S.C.	9	3.26	9.86	1.08	57.2	2.4	600-1000
Al_2O_3 sintered	7	7.35×10^{-2}	0.247	2.19×10^{-2}	43.8	2.5	600-900
BeO S.C.	14	1.11×10^{-2}	8.91×10^{-2}	1.39×10^{-3}	52.5	4.7	650-1200
BeO sintered	11	7.00×10^{-2}	0.445	1.10×10^{-2}	48.5	3.6	500-950
Lucalox (MgO doped Al_2O_3)	15	39.8	357	4.43	41.8	3.2	360-570
α - SiC S.C.	12	1.09×10^{-2}	2.92×10^{-2}	4.05×10^{-3}	54.9	2.5	700-1300
β - SiC S.C.	10	28.0	172	4.55	65.0	4.1	750-1000
Al-doped α - SiC S.C.	8	4.04×10^{-4}	3.80×10^{-3}	4.29×10^{-5}	34.0	4.2	450-950
Al-doped hot-pressed α - SiC	11	0.904	6.68	0.147	48.2	3.5	500-800
SCB glass	10	2.95×10^{-4}	6.34×10^{-4}	1.37×10^{-4}	30.2	1.2	350-800
Y_2O_3 hot-pressed	8	0.431	7.13	2.6×10^{-2}	39.1	4.3	420-620
Yttralox	6	3.87	32.2	0.464	39.5	3.1	350-600
Si-doped PyC	14	1.1×10^{-3}	3.9×10^{-3}	3.1×10^{-4}	53.6	3.5	800-1300
LTI Pyrolytic Carbon	7	4.4×10^{-6}	-	-	32.0	-	800-1200
Laminar Pyrolytic Carbon	9	3.3×10^{2}	2.0×10^{4}	5.4×10^{1}	98.4	5.7	1150-1400
Si_3N_4	14	0.122	-	-	52.1	-	600-1000
B_4C	14	1.12×10^{-6}	-	-	16.8	-	300-700
KT SiC (from permeation studies)	33	3.61×10^{2}	-	-	59.5	-	1150-1450

Hydrogen diffusion results in sintered alumina tubes were also obtained by the techniques described in Section I.C. under Experimental Techniques. The diffusion coefficients obtained were at much higher temperatures than the recoil injection experiments and it was necessary to extrapolate results for comparison. Figure 8 presents the diffusion coefficients obtained during temperature transitions in the permeation experiments for alumina as compared with the extrapolated diffusion results for sintered and single-crystal alumina. The agreement is within the experimental error anticipated for experiments of this nature.

It is of interest that the permeation experiments yielded interpretable diffusion results only when the temperature was increased from a low to a higher temperature and not for the reverse case. The reasons for this anomaly are unknown but possible explanations have been presented in a recent publication[7].

Hydrogen solubility measurements in alumina proved difficult to make as the solubilities were near the sensitivity limit for mass spectrometric detection. Measurements were made with single-crystal alumina and powdered specimens but it is recognized that considerable uncertainty exists with the measurements. An additional complication was the necessity for correcting for absorbed hydrogen in the solubility measurements.

The measured hydrogen solubilities corrected to a hydrogen pressure of one atmosphere are presented in Figure 9. The expression best fitting all experimental results is tabulated in Table III. A best-fit solubility expression that includes results from the present study and the paper by Roy and Coble[8] is also included.

Hydrogen permeation studies were conducted with high-density, sintered alumina tubes. Reproducible permeation results could be obtained and are presented in Figure 10. Under ideal conditions the permeation of a solid can be expressed as a product of the solubility and diffusivity. For this condition:

$$K(\text{permeability})(\text{atoms sec}^{-1}\text{cm}^{-1}\text{atm}^{-n}) = S(\text{solubility})(\text{atoms cm}^{-3}\text{atm}^{-n}) \times D(\text{diffusivity})(\text{cm}^2\text{sec}^{-1}) \quad (4)$$

Also included in Figure 10 is the calculated permeability curve based upon the best-fit solubility and diffusivity results. The two curves are in generally good agreement.

Hydrogen permeation as a function of hydrogen pressure was investigated over the pressure range 0.02 atm to 0.5 atm. The pressure dependence of permeability is consistent with an expression of the form:

$$K \sim P^{0.43} \qquad P=\text{pressure} \tag{5}$$

The following equation represents hydrogen permeability of alumina where both pressure and temperature effects are included.

$$\phi(\text{Hatoms-cm-cm}^{-2}\text{-sec}^{-1}) = P^{0.43} \exp\{50.80 \pm 1.34\} \exp\{-76.0 \pm 4.5 \text{kcal-mol}^{-1}/RT\} \qquad P=\text{pressure (atm)} \tag{6}$$

II. Silicon Carbide (SiC)

Tritium diffusion measurements through recoil injection were conducted with single-crystal, vapor-deposited, hot pressed and sintered specimens of silicon carbide. Table II summarizes the diffusion parameters observed and the temperature ranges of measurement while Figure 11 plots the experimental results. Single-crystal specimens containing aluminum impurity exhibited significantly higher diffusion coefficients than undoped specimens, a result in agreement with the impurity effect noted for MgO-doped alumina. The diffusion results for single-crystal specimens from different sources are in substantially good agreement but differences of several orders of magnitude were observed between other specimens. These disparities reflect differences in specimen morphology and are discussed further in the Discussion section. The diffusion coefficients determined from the KT-silicon carbide tubes used in the permeation experiments were much larger than the values obtained through recoil injection and these values have been presented in Figure 12.

Deuterium solubilities in alpha silicon carbide powder and vapor-deposited beta silicon carbide were measured as a function of temperature and the results are presented in Figure 13 and Table III. It is of interest to note that the solubility of deuterium in both materials decreased with increasing temperature, leading to a negative value for the heat of solution. Also included in the Figure are solubilities determined from the permeation experiments as described

TABLE III

MEASURED SOLUBILITIES FOR DEUTERIUM IN Al_2O_3, SiC AND PYROLYTIC CARBON

$$S(\text{atoms } g^{-1}) = So \exp(-\Delta H/RT)$$

Material	So	ΔH (kcal-mol^{-1})	Temp.Range
Al_2O_3 [1]	2.03×10^{21}	20.8	700-1816
β-SiC (vapor deposited)	1.32×10^{14}	-37.1	1000-1400
KT-SiC (sintered)	2.56×10^{15}	-33.3	1100-1500
Pyrolytic Carbon (laminar)			

[1] Curve fit includes data generated by Roy and Coble (Ref. 8).

in Section II.B. in the Experimental Procedures.

Figure 14 presents the dependence of hydrogen solubility on pressure at 1200 degrees C. As with alumina, solubility is not a linear function of hydrogen pressure and the power dependence is similar to the 0.5 value expected for atomic hydrogen dissolution.

Figure 15 includes the permeation results obtained for high density, KT silicon carbide tubes. Also included in the Figure are two calculated permeabilities. Curve A is the calculated permeability utilizing the β-SiC single-crystal diffusivity data and the results for vapor deposited, β-SiC for hydrogen solubility. Curve B is based on all measured results for KT silicon carbide with the diffusivity values deriving from the temperature change release kinetics of permeability and the solubilities from the end of experiment release results of dissolved hydrogen. The calculated permeabilities for SiC obtained from both sets of solubilities and diffusivities are in excellent agreement with the measured permeability. Thus for both Al_2O_3 and SiC, there is good agreement among measured values of diffusivity, solubility and permeability.

Figure 16 gives the measured dependence on hydrogen partial pressure for permeability at 1250°C. The curve shows that hydrogen permeability of the KT silicon carbide exhibits a near square-root dependence as does the solubility data for SiC. The following equation is analogous to equation (6) for alumina and represents hydrogen permeability of KT silicon carbide where both temperature and pressure effects are included:

$$\phi(\text{Hatoms-cm-cm}^{-2}\text{sec}^{-1}) = P^{0.40}\exp\{49.33\pm1.50\}\exp\{-67.6\pm4.55\text{kcal-mol}^{-1}/RT\} \quad P=\text{pressure in atm, } 1150C\leq T\leq 1450C \qquad (7)$$

III. Pyrolytic Carbon

Diffusion measurements by tritium recoil injection were conducted with LTI pyrolytic carbon, a laminar pyrolytic carbon and silicon-doped pyrolytic carbon. The diffusion results are presented as Arrhenius plots in Figure 17 and the least-squares, best-fit parameters are presented in Table II. Included in the Figure is a measured diffusion curve for beta silicon carbide that shows excellent agreement with the curve for silicon-doped pyrolytic carbon.

In the absence of hydrogen in the external sweep gas, the release results from pyrolytic carbon were found to be desorption rate controlled. Figure 18 presents observed diffusion results for LTI pyrolytic carbon with a helium sweep gas only and subsequently with hydrogen added to the sweep gas.

Substantial difference is observed. All results in Figure 17 were subsequently taken with a hydrogen sweep gas and it is believed that these results represent diffusion controlled release although surface effects remain possible. To verify the diffusion results obtained by the release experiments, layers were electropolished from injected carbon specimens using an etch of mercuric sulfate (133 mg), concentrated H_2SO_4 (10 ml), CrO_3 (10 g) and H_2O (25 ml) at 140°C[9]. The tritium removed by etching was distilled from the solution as tritiated water and counted in a liquid scintillation counter to determine concentrations. The validity of the technique was demonstrated by reproducing the recoil concentration profile without specimen heating. Figure 19 shows typical tritium profiles for various times and temperatures. These results exhibited considerable scatter but were generally consistent with the diffusion release results as shown by the etching experiment results in Figure 17. Tritium release results with hydrogen in the gas sweep stream, therefore, appear to give valid diffusion results for tritium transport.

Deuterium dissolution experiments were conducted as a function of time and deuterium concentration. The low diffusion coefficients in pyrolytic carbon prevented the attainment of dissolution equilibrium and it was necessary to estimate the percent of equilibration from a knowledge of diffusion coefficients and the calculated diffusion profiles based upon the assumption that kinetic barriers for surface dissolution were absent. This approach is less satisfactory than previously employed methods that involved complete dissolution equilibrium as errors are possible in the determination of percent dissolution equilibration. Figures 20 and 21 summarize the temperature and pressure effects observed. The pressure effect is again much more suggestive of atomic rather than molecular hydrogen dissolution and the power dependence of deuterium pressure of 0.49 is extremely close to the 0.50 expected for atomic dissolution. No permeation measurements were conducted for pyrolytic carbon materials.

IV. Beryllium Oxide (BeO)

Only diffusion studies were conducted for all of the following materials, and no solubility or permeation data were obtained. This was principally a consequence of time limitations in the experimental studies but was also due to difficulty in obtaining reproducible results or satisfactory specimens. For example, efforts were made to measure solubility in beryllium oxide and these were not successful. The apparent hydrogen solubilities appeared to be below the detection sensitivity of the mass spectrometer technique ($<\sim 10^{17}$ atoms g^{-1}).

Tritium diffusivities through recoil injection were measured with single-crystal, sintered, and powdered beryllium oxide specimens. All diffusion

results are presented in Figure 22 and in Table II along with a single best-fit result for BeO specimens. The agreement between results was generally satisfactory except that the powders appeared to exhibit considerable experimental scatter and the measured diffusion activation energies were somewhat lower than the values obtained for bulk specimens. As with alumina, a considerable fraction of the released tritium appeared in condensible form, presumably as tritiated water. Slightly different values of diffusion coefficient and activation energy were obtained when these condensibles were removed, as shown in Figure 23, but the difference was not sufficient to warrant the trapping of condensibles in all experiments. This observation suggests that the incorporation of tritium in condensible form or its release from a specimen is not a rate controlling step in the diffusion process.

V. SCB Glass (SiO_2)

Considerable data exist in the literature on the transport of hydrogen in various types of glasses[10-14] and only nominal investigation was, therefore, undertaken in the present study. A high Ba-Ti glass developed by Atomics International as a hydrogen barrier for SNAP reactors was of particular interest and recoil injection measurements were made for tritium diffusion. These results are presented in Figure 24.

VI. Yttrium Oxide (Y_2O_3)

Yttria was at one time under consideration as a potential insulator in fusion reactors and was investigated in the present program since little data exist for rare earth oxides. The hot-pressed specimens studied were assumed to have no internal porosity that might produce rapid conduction paths to the surface and the measured diffusion coefficients should, therefore, be regarded as upper limits. Figure 24 presents the diffusion results for this material. Data were also taken for Yttralox, a thorium-doped yttria available from General Electric Co. These data are included in the figure.

VII. Silicon Nitride (Si_3N_4)

Silicon nitride was of interest in the study as it has been considered for a fusion blanket insulator and because very few data exist on hydrogen transport in nitrides. Measurements were taken for both sintered and powdered specimens but the powder results exhibited considerable scatter and have not been included. Figure 25 presents the results observed for tritium diffusion

in sintered silicon nitride. As with the studies on alumina and BeO powders, the tritium released from silicon nitride powder was largely in condensible form and was likely a factor in producing erratic results.

VIII. Boron Carbide (B_4C)

Boron carbide is a neutron absorber planned for use in control rods for fast reactors such as the FFTF. Tritium production occurs through the reactions:

$$^{10}B(n,{}^{3}H)^{8}Be$$

$$^{11}B(n,{}^{3}H)^{9}Be$$

$$^{10}B(n,2\alpha)^{3}H$$

$$^{10}B(n,\alpha)^{7}Li(n,n\alpha)^{3}H$$

Tritium can be released to the reactor coolant through diffusion. Tritium production and release remains a potential problem in fast breeder reactors so the boron carbide was studied as a basis for potential release measurements of tritium in fast reactor control rods. Samples were obtained from HEDL in Richland, Washington and the diffusion results are presented in Figure 26.

DISCUSSION

I. Non-Metallics as Tritium Diffusion Barriers

All of the measured diffusion coefficients for non-metallic solids were many orders of magnitude lower than the diffusion coefficients reported in the literature for the refractory metals most frequently considered as first wall blanket materials (Nb, W, Mo, S.S.). This result suggests that the materials studied could be effective tritium barriers if a suitable method of deposition could be devised and if coating integrity could be maintained during actual operation. An estimate of effectiveness can be obtained by assuming that the concentration of diffusing tritium is uniform across a barrier-substrate interface. An alternative statement of this assumption is that the partition coefficient of hydrogen at the interface is unity. For this case, a simple expression can be derived for the equilibrium release rate of tritium from a substrate with a coating divided by the equilibrium release rate for the same substrate without a coating. The equation for release rate inhibition is given by:

$$\frac{R'}{R} = \frac{\text{Eq. Release Rate (w coating)}}{\text{Eq. Release Rate (w/o coating)}} = \frac{\left(\frac{X_1}{D_1}\right)}{\left(\frac{X_2}{D_2}\right)+\left(\frac{X_1}{D_1}\right)} \qquad (8)$$

D_1, D_2 = Diffusion coefficients in substrate and coating, respectively, $(cm^2 sec^{-1})$

X_1, X_2 = Thickness of substrate and coating (cm).

Table IV tabulates the quantity $-\log_{10}(R'/R)$ for the coating materials studied and four metal substrates--molybdenum, stainless steel, tungsten and niobium. It is apparent that a pronounced lowering in equilibrium permeation rate can be attained if coatings without short circuit paths to the surface could be prepared.

A more directly related appraisal of tritium barrier effectiveness may be obtained from the actual measured permeation rates and from those permeation rates that can be calculated from solubility and diffusivity data. Figure 27 tabulates the permeabilities of the four mentioned metals as a function of temperature for the hydrogen partial pressure stated. The same figure includes

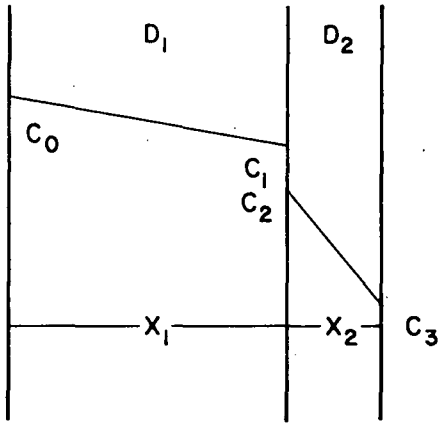

METAL COATING

IF:

$C_1 = C_2$

$C_3 = 0$

SYSTEM AT EQUILIBRIUM

THEN:

$$\frac{R'}{R} = \frac{\text{EQ. RELEASE RATE - COATING}}{\text{EQ. RELEASE RATE - NO COATING}} = \frac{\left(\frac{X_1}{D_1}\right)}{\left(\frac{X_2}{D_2}\right)+\left(\frac{X_1}{D_1}\right)}$$

FOR T = 600°C $X_1 = 0.2$ cm $X_2 = .01$ cm $\left(-\log \frac{R'}{R}\right)$

COATINGS	W	Mo	Nb	S.S.(Aust.)
Al_2O_3	6-8	6-7	7-8	6-7
BeO	7-9	7-9	8-10	7-9
Y_2O_3	4	4	5	4
SiC	6-10	6-9	7-10	6-9
LUCALOX	3	2	3	2
YTTRALOX	3	3	4	3
SCB GLASS	5	5	6	5
PyC	16	16	17	16

TABLE IV EFFECTIVENESS OF NONMETALLIC COATINGS AS TRITIUM BARRIERS BASED UPON MEASURED DIFFUSION COEFFICIENTS

measured permeabilities of alumina and silicon carbide tubes plus the permeabilities calculated for these two materials and pyrolytic carbon based upon solubility and diffusivity measurements. It is again apparent that the permeabilities of the non-metallic solids are well below those measured for refractory metals at most temperatures.

It is unfortunate that it was not possible to actually deposit metal-oxide or carbide coatings on metal substrates and evaluate their performance in the present study. This would be an appropriate next step but would involve an effort considerably greater than that devoted to the present program.

II. Permeation Results

The purpose of the permeation studies with commercially available specimens of alumina and silicon carbide was to determine if off-the-shelf, high density sintered materials could give permeabilities similar to those determined from diffusivity and solubility measurements or if a sufficient number of short-circuit diffusion paths were created by open porosity to give entirely different transport behavior. Figure 10 shows that the permeabilities measured for high-density, sintered alumina were in excellent agreement with those values calculated from solubility and single-crystal diffusivity results. This result indicates that hydrogen transport through diffusion and dissolution within crystallite grains is rate controlling rather than diffusion through open porosity within the tube walls. The results also support the diffusivity and solubility numbers reported in the test.

Similar agreement between calculated and observed hydrogen permeation was observed for silicon carbide. The permeabilities calculated from both the KT-SiC solubility and diffusivity data and the single-crystal diffusivities and β-SiC solubilities were in surprisingly good agreement with measured permeabilities. This may be coincidental as the measured KT-SiC solubilities were several orders of magnitude below the values for β-SiC while the diffusivities for KT-SiC were several orders of magnitude above the corresponding values for single-crystal SiC. Therefore, the products of S(solubility) x D(diffusivity) were in good agreement for the two cases considered even though the contributing terms showed much larger variations.

The high values for diffusivity in KT-SiC likely reflect internal porosity within the tubes which increases the effective surface area in the diffusivity

calculation to values higher than the geometric surface area used in the calculation. It is not unexpected that the apparent KT-SiC diffusivities would be higher than values for single-crystal material as the geometric surface area would be expected to underestimate the true surface area.

The disagreement in solubilities raises questions about the methods used to determine hydrogen solubility in the β-SiC specimens. These specimens were too massive to obtain equilibrium hydrogen dissolution and the diffusion coefficients were used to calculate the degree of equilibration and the true solubility. The disagreement between these values and the solubility values measured for KT-SiC suggests that this is perhaps an unacceptable method that does not adequately account for kinetic barriers to dissolution.

Above 1375°C, the hydrogen permeability values in KT-SiC show a sudden increase. This temperature approximately coincides with the melting point of silicon, and the increased permeability is believed to be due to melting of the free silicon which gave rise to fast diffusion paths. Inspection of KT-SiC tubes that had been heated to elevated temperatures showed beads of condensed Si on the cooler tube surfaces so the distribution of free silicon clearly changed during the high temperature permeation studies.

One conclusion from the permeation results is that it should be possible to develop coatings of non-metallic inorganic solids that would have lower tritium permeabilities than the substrate metals under initial preparation conditions. Whether such coatings would maintain integrity over temperature cycling and long time periods is a subject for considerable additional study.

III. Comparisons with Literature Results

Differences greater than experimental error were observed in this study between different specimens of the same material. This is not unexpected when one considers that special problems can arise in treating release data from powdered specimens and the sintered bodies were treated as monolithic solids with no accelerated diffusion along grain boundaries. General agreement was obtained between single-crystal specimens of materials of the same compound and the disparity with sintered specimens was not generally large. Very little data exist in the literature to allow comparisons of these results. A review[10] prepared under the present contract of all hydrogen transport properties in non-metallic inorganic solids compares the present results with results obtained by other investigators. These comparisons show that the dif-

fusion data in alumina are in approximate agreement with the results reported by Hauffe and Hoeffgen[15] and by Roberts and Roberts[16] (see Figure 28). Measurements were made over different temperature intervals and extrapolation is required for comparison. The diffusion results for s.c. beryllium oxide in the present study are in excellent agreement with the diffusion results in single-crystal BeO reported by Scott and Wassell[17], and for compacts by Rothwell and Wassell[18], but are in less satisfactory agreement with the powder results presented by Palmer, Roman and Whitfield[19] and Scott and Wassell[17] (see Figure 29). Diffusion results for silica were in agreement with a large body of the silica diffusion studies as summarized in Reference (10). Hydrogen solubility in alumina measured in the present study was in satisfactory agreement with the values extrapolated from the data of Roy and Coble[8]. No other data in the literature was found to allow comparisons with the present results. It would appear from the above examples, however, that there is sufficient indication of agreement to place reasonable reliance in the results in making estimates of transport parameters for initial design purposes.

The large negative heat of solution for deuterium in beta silicon carbide leads to high extrapolated solubilities at lower temperatures. These extrapolated solubilities imply that large inventories of tritium could exist in silicon carbide in the blanket region of fusion reactors. The occurrence of a negative heat of solution is consistent with the presence of chemical bonding effects between the hydrogen atoms and the host lattice atom during dissolution. At higher temperatures the ability of the hydrogen atoms to break the bonds and escape from the material become greater and results in a decrease in the solubility.

Data in the literature show that injected hydrogen atoms in metal oxides form a significant percentage of hydroxyl bonds,[20,21] so it is likely that carbon-hydrogen compound formation could occur in metal carbides. The observed excellent agreement between hydrogen diffusion coefficients in pyrolytic carbon and in silicon carbide suggests that carbon-hydrogen bond formation may occur in both materials. Negative heats of solubility were also observed for dissolution in carbon as summarized in Figure 20.

IV. Impurity Effects

Diffusion measurements using tritium recoils were conducted in two solids

with relatively large impurity concentrations (MgO-doped alumina and Al-doped silicon carbide). In both cases, the tritium coefficients were well above those values observed for the corresponding undoped materials. The results suggest a rather strong impurity effect on hydrogen transport that could be important in fusion reactor blankets. Since transmutation reactions in the blanket result in significant impurity introductions over time, this effect could alter hydrogen transport behavior in some blanket regions. One explanation for the impurity effect assumes that hydrogen diffuses interstitially with cation vacancies acting as traps. Impurities that occupy these traps and lowered vacancy concentrations would yield higher observed hydrogen diffusion rates.

V. Chemical Form of Dissolved and Diffusing Hydrogen

The tritium injected into specimens in the recoil diffusion experiments was present in concentrations sufficiently low that a diffusing H atom would encounter a free surface before another tritium atom. The tritium was known to be injected as individual atoms so the measured diffusion coefficients apparently measure the diffusion behavior of atomic rather than molecular hydrogen. An uncertainty in this conclusion must be recognized since the presence of even several parts per million of dissolved hydrogen would be sufficient to allow the formation of hydrogen molecules.

The dissolution of hydrogen as molecular hydrogen would be expected to yield a linear relation between solubility and hydrogen partial pressure while dissolution as atomic hydrogen would have a square-root pressure dependence, consistent with the familiar Sievert's Law behavior encountered in metals. The deuterium dissolution results for silicon carbide and pyrolytic carbon gave a pressure dependence that is closer to that expected for atomic rather than molecular hydrogen. In the case of pyrolytic carbon, the observed pressure dependence was almost exactly the 0.5 expected for atomic diffusion. Also the permeability pressure dependence for alumina is consistent with atomic rather than molecular diffusion.

Additional evidence in the literature support the dissolution of hydrogen in non-metallic solids as atomic rather than molecular hydrogen. Roberts[22] studied hydrogen permeation in alumina with and without electric fields and observed an effect which suggested that hydrogen moved as protons rather than molecular hydrogen. Mollwo[28] has investigated hydrogen solubility in zinc

oxide single-crystals at partial pressures from one to twenty atmospheres and has observed a square root pressure dependence that is consistent with hydrogen dissolution as atomic hydrogen. Thomas and Lander[24] have measured hydrogen diffusion coefficients in ZnO using changes in electrical conductivity to monitor hydrogen concentrations in the crystals. The model for the electrical conductivity change supports atomic rather than molecular hydrogen. Wagner[25] has investigated the kinetics of H_2O vapor dissolution in ZrO_2-Y_2O_3 solid solutions and has concluded that hydrogen diffusivities are consistent with molecular dissociation to form protons. In studies of the tungsten bronzes (H_xWO_3) Dickens, et al[26] observed that hydrogen dissolved in the lattice appeared to become attached to oxygen atoms as hydroxyl groups, a process that is consistent with hydrogen dissociation. Although some investigators have interpreted hydrogen transport results in terms of molecular diffusion (for example, see Caskey[27]) the predominant evidence implies that hydrogen exists in some metal oxides as atomic rather than molecular hydrogen.

VI. Chemical Form of Released Tritium

It was noted in the studies with powdered specimens that large percentages of released tritium were frequently in condensible form, presumably as tritiated water. In alumina and beryllia powders, 70 to 95 percent of the released tritium was found to be condensible. Similar results were obtained with the silicon nitride powders where as much as 95% of the released tritium could be retained in a cold trap. Specimens with larger particle sizes exhibited lower percentages of condensible tritium. For example, the sintered or single-crystal alumina specimens typically exhibited only 0 to 25% condensible tritium. Drying of alumina powders at elevated temperatures for extended time periods prior to irradiation and subsequent storage in dry atmospheres decreased the percent of condensible tritium released from 95% to 37% at 700 degrees C., indicating that exchange with absorbed water was one factor in the tritiated water released.

Other investigators have commonly observed tritium release in condensible form. Rothwell and Wassell[18] and Scott and Wassell[17] have observed that a significant fraction of the tritium released from BeO powders was condensible, presumably as tritiated water. Nasu, et al[2] have extensively studied the chemical form of hydrogen released from irradiated lithium oxide pellets. They

observed that substantially all of the released tritium was condensible. Aratono and Tachikawa[3] and Scargill[28] both observed release of major fractions of tritium from UO_2 as tritiated water vapor. Aratono and Tachikawa[3] extensively studied the chemical form of release tritium and concluded that the fraction of tritium in water vapor was a strong function of the sweep gas water concentration and approached 100% as water was added to the sweep stream. The authors concluded that HTO was likely the diffusing species in UO_2 and that reduction to HT occurred near the specimen surface, followed by later surface or gas stream exchange with water vapor. Hydrogen reactions other than water formation occurred in solids to form small percentages of other volatile compounds. Aratono and Tachikawa[3] observed a release of less than .01% of the tritium as $C(^3H)_3T$. Nasu, et al[2] observed from 0.3-1.5% of the tritium coming from lithium oxide as methane and small percentages (0.5 to 1.4%) as ethylene and acetylene.

The results of the present study are most consistent with a model that assumes exchange of diffusing tritium with absorbed water on the specimen near the surface. The addition of large concentrations of hydrogen to the sweep gas did not completely eliminate the presence of tritiated water vapor in the sweep gas, as would be expected if gaseous exchange within the sweep gas was the sole mechanism for tritium incorporation in water. It, therefore, appears that tritium is in the water form at the time of release from the specimen and is not exchanged with water after release. The observation that drying of the specimens reduced the percent of tritium appearing as water vapor is consistent with the explanation involving exchange with absorbed water. It does not appear reasonable in our studies that the hydrogen diffuses as water vapor or that water vapor formation with tritium is involved in the rate determining steps for diffusion and release. This conclusion is supported by the observation that the diffusion coefficients obtained for alumina and beryllia powders both with and without trapping of the condensible tritium fractions were quite similar. This observation would not be expected if transport of tritiated water vapor were rate limiting. The observation of tritiated hydrocarbons in gas release stream raises intriguing questions on the chemical forms of transported tritium in fusion reactors and further study of this subject appears warranted.

VII. Powder Effects

The diffusion coefficients obtained in this study were least in agreement when powdered specimens were compared against results measured for sintered or single-crystal specimens. A similar result is observed in the literature. For example, Scott and Wassell[17] observed tritium diffusion coefficients for irradiated BeO powder that were in considerable variance with their results for single-crystal specimens. A number of explanations can be offered for this disparity in results. Experiments with powders are naturally suspect because of difficulties in the measurement of accurate surface areas and problems associated with the release of surface absorbed hydrogen which can be incorrectly interpreted as diffusion release. Lehovec[29] and DeFord and Johnson[30] have discussed the potential importance of internal electric fields involving non-metals. The latter workers concluded that internal fields can produce errors of 10 or even a 100 in measured diffusion coefficients. This effect increases in importance with increasing specimens surface area and would be most important with powders. Another potential source of error with powders concerns the assumption that powder particles are all of the mean particle radius whereas they are actually distributed in size. Tritium release rates from small particles decreases rapidly to zero to give an apparent release rate at intermediate times that is below the predicted rate for uniform particles. Since an increasing fraction of particles is depleted as the temperature increases, this effect could contribute to an observed low activation energy with powders.

The presence of alternate crystal structures in powders could also affect release results. The X-ray diffraction spectra of the alumina powder used in the present study showed the presence of a gamma phase in addition to the alpha phase, and this could significantly alter tritium release characteristics.

In view of the many potential sources of error for diffusion measurements in powders, it is perhaps to be expected that the observed disparities with other specimens would exist. It would appear that it is desirable to avoid the use of powder specimens in the conduct of diffusion studies where this is possible.

CONCLUSIONS

The following conclusions may be drawn from the present study:

1. In the few cases where comparisons with other work is possible, the diffusion and solubility results for the present study are in general agreement with other work reported in the literature.

2. The measured diffusivities and the permeabilities measured directly or calculated from diffusion and solubility results suggest that non-metallic solids could be effective tritium barriers if their transport properties could be maintained over time in thin coatings.

3. The measured hydrogen solubilities in silicon carbide and pyrolytic carbon increased with decreasing temperatures and attained atom fractions at low temperature in considerable excess of the solubilities determined for refractory metals. It is possible that relatively high hydrogen inventories could build up in these materials at low temperatures. The one oxide measured (alumina) exhibited a positive rather than a negative heat of solution and had low hydrogen solubility over the entire temperature range measurement.

4. The experimental results are more consistent with hydrogen diffusion and dissolution as atomic rather than molecular hydrogen.

REFERENCES

1. DiCola, G. and H. Matzke, Nucl. Instrum. Methods 57(2) 341-45 (1967).

2. Nasu, S., H. Kudo, K. Shiozawa, T. Takashashi, T. Kurasaw, M. Tachiki and K. Tanaka, J. Nucl. Mat. 68:261-4 (1977).

3. Aratono, Y. and E. Tachikawa, J. Inorg. Nucl. Chem. 39:2125-2130 (1977).

4. Shewmon, P. G., Diffusion in Solids, pp. 145-50, McGraw-Hill (1963).

5. Jost, W., Diffusion in Solids, Liquids, and Gases, Academic Press, N.Y. (1960).

6. Fowler, J. D., D. Chandra, T. S. Elleman, A. W. Payne and K. Verghese, J. Am. Ceram. Soc. 60:No. 3-4, 155-161 (1977).

7. Roberts, R. M., T. S. Elleman, H. Palmour and K. Verghese, J. Am. Ceram. Soc. (accepted for publ.)(1979).

8. Roy, S. K. and R. L. Coble, J. Am. Ceram. Soc. 50:No. 8, 435-6 (1967).

9. Engelhard, J., "Studies on the Diffusion of Metallic Fission Products and Heavy Metals in the Coatings of Fuel Particles for High Temperature Reactors" USAEC Report JUL-752-RG(1971).

10. Elleman, T. S., D. Rao, K. Verghese, and L. Zumwalt, "Hydrogen Diffusion, Dissolution and Permeation of Nonmetallic Solids" to be published as a DOE report.

11. Doremus, R. H., Glass Science, John Wiley & Sons, N. Y. (1973).

12. Lee, R. W., Physics and Chemistry of Glasses, Vol. 5, No. 2, pp. 35-43, (1964).

13. Lee, R. W. and D. L. Fry, Physics and Chemistry of Glasses, Vol. 7, No. 1, pp. 19-28 (1966).

14. Shelby, J. E., J. Appl. Phys. 48:No. 8, pp. 3387-94 (1977).

15. Hauffe, K. and D. Hoeffgen, Ber. Bunsenges Phys. Chem. 74:537-46 (1970).

16. Roberts, E. W. and J. P. Roberts, Bull. Soc. Fr. Ceram. No. 77:2-13 (1967).

17. Scott, K. T. and L. L. Wassell, Proc. Brit. Ceram. Soc. 7:375-80 (1967).

18. Rothwell, E. and L. L. Wassell, J. Nucl. Mat. 16:208-14 (1965).

19. Palmer, A. R., D. Roman and H. J. Whitfield, J. Nucl. Mat. 14:141-6 (1964).

20. Behrisch, R., R. S. Blewer, J. Borders, R. Langley, J. Roth, B. M. U. Scherzer and R. Schulz, "Implantation of 5 keV Deuterium in BeO" Int. Conf. on Ion Beam Modification of Materials, Budapest (1978).

21. Gruen, D. M., R. B. Wright, R. L. McBeth, and I. Sheft, J. Chem. Phys. 62(3) 1192-93 (1975).

22. Roberts, E. W., Science of Ceramics, 7:318-339 (1973).

23. Mollwo, E., Z. Physik 138:478 (1954).

24. Thomas, D. G. and J. J. Lander, J. Chem. Physics 25:No. 6 1136-42 (1956).

25. Wagner, C., Ber. Bunsenges Phys. Chem. 72:No. 7, pp. 778-81 (1968).

26. Dickens, P. G., D. J. Murphy and T. K. Halstead, J. Solid State Chem. 6:370-373 (1973).

27. Caskey, G. R., Materials Science and Engineering 14:109-14 (1974).

28. Scargill, D., J. Nucl. Mat. 74:62-7 (1978).

29. Lehovec, K., J. Chem. Phys. 21(7) 1123-28 (1953).

30. DeFord, J. W. and O. W. Johnson, J. Appl. Physics 46:No. 3, 1023-5 (1975).

Appendix A

Publications Resulting from Program

1. T. S. Elleman and K. Verghese, "Tritium Diffusion in Fusion Reactor Materials", Proceed. Symposium on Tritium Technology Related to Fusion Reactor Systems, Oct. 1-2, 1974, Mound Laboratory, Miamisburg, Ohio, ERDA-50 (1975).

2. J. D. Fowler, R. A. Causey, D. Chandra, T. S. Elleman, and K. Verghese, "Tritium Diffusion in Ceramic Materials for Thermonuclear Reactors", J. Vac. Sci. Technol. 13:No. 1, p. 401, Jan./Feb. 1976.

3. T. Elleman, C. Alexander, R. Causey, D. Chandra, J. Fowler, C. Ravanbakht, L. Zumwalt and K. Verghese, "Tritium Transport in Nonmetallic Solids" Proceed. Meeting on CTR Electrical Insulators, Los Alamos, N. Mex., May 17-19 (1976), CONF-760558 (1978).

4. J. D. Fowler, R. A. Causey, D. Chandra, T. S. Elleman and K. Verghese, "Tritium Diffusion in Ceramic CTR Materials" Conf. on Radiation Effects and Tritium Technology for Fusion Reactors, Gatlinburg, Tenn., October 1-3, 1975, CONF-750989, Vol. IV (1976).

5. J. D. Fowler, D. Chandra, T. S. Elleman, A. W. Payne, and K. Verghese, "Tritium Diffusion in Al_2O_3 and BeO" J. American Ceram. Soc. 60:No. 3-4, 155-161 (1977).

Reprint Removed

6. R. A. Causey, J. D. Fowler, C. Ravanbakht, T. S. Elleman and K. Verghese, "Hydrogen Diffusion and Solubility in Silicon Carbide", J. Am. Ceram. Soc. 61:No. 5-6, 221-225 (1978).

7. R. M. Roberts, T. S. Elleman, H. Palmour III and K. Verghese, "Hydrogen Permeability of Sintered Aluminum Oxide" J. Amer. Ceram. Soc. (to be published)(1979).

8. T. S. Elleman, L. R. Zumwalt and K. Verghese, "Hydrogen Transport and Solubility in Nonmetallic Solids" Conf. on the Technol. of Controlled Nuclear Fusion, Sante Fe, N. Mex., May 9-11, 1978:CONF-780508, pp. 763-770.

9. R. A. Causey, T. S. Elleman and K. Verghese, "Hydrogen Diffusion and Solubility in Pyrolytic Carbon" Carbon (to be published)(1979).

10. K. Verghese, L. R. Zumwalt, C. P. Feng and T. S. Elleman, "Hydrogen Permeation Through Non-Metallic Solids", First Topical Meeting on Fusion Reactor Materials, Jan. 29-31, 1979, Miami Beach, Florida (Proceedings to be published).

11. T. S. Elleman, et al., "Tritium Diffusion in Non-Metallic Solids of Interest for Fusion Reactors" Annual Progress Reports, USDOE Report ORO-4721-1 through ORO-4721-4.

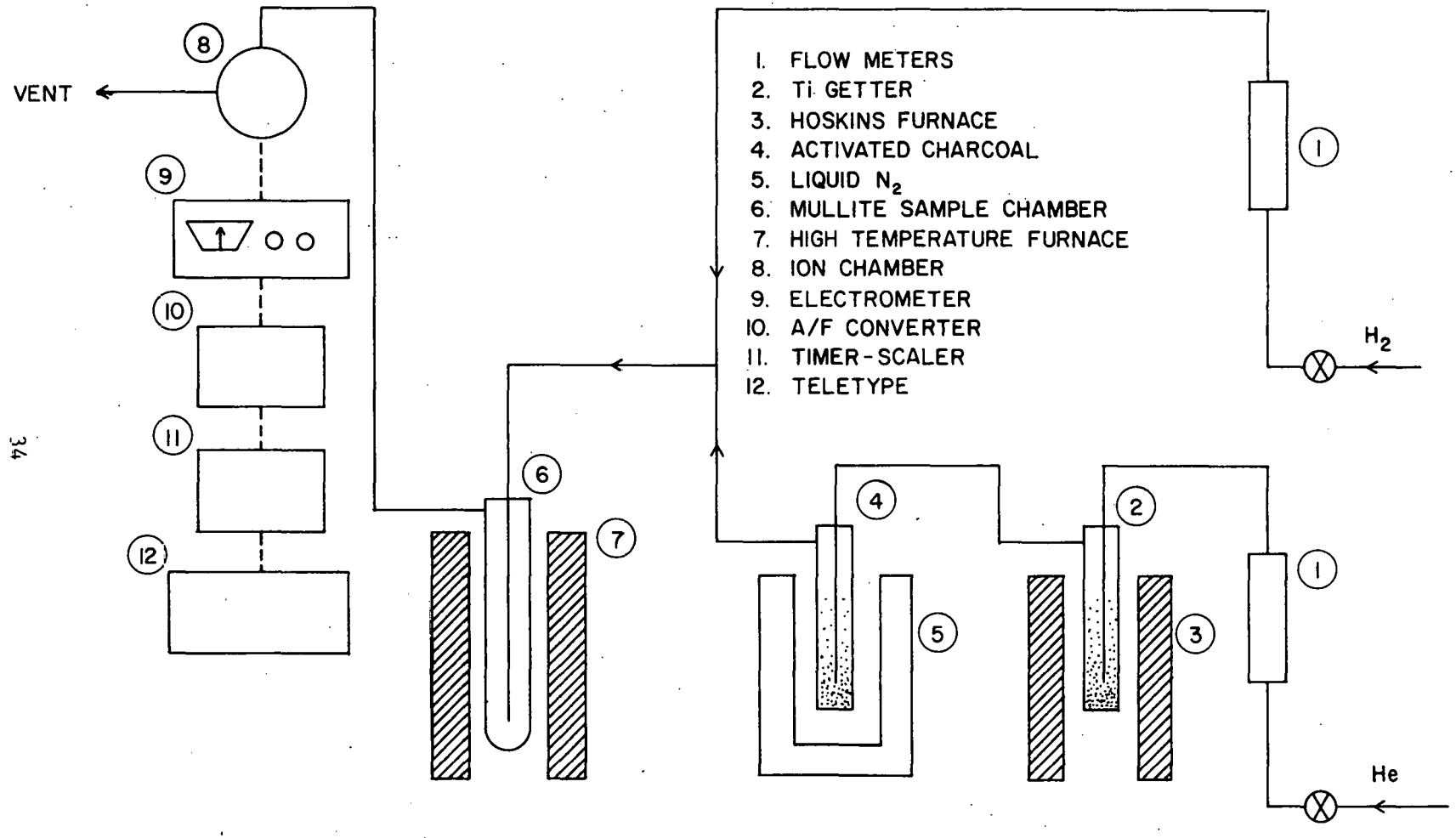

FIGURE 1

GAS-RELEASE SYSTEM USED FOR TRITIUM DIFFUSION MEASUREMENTS

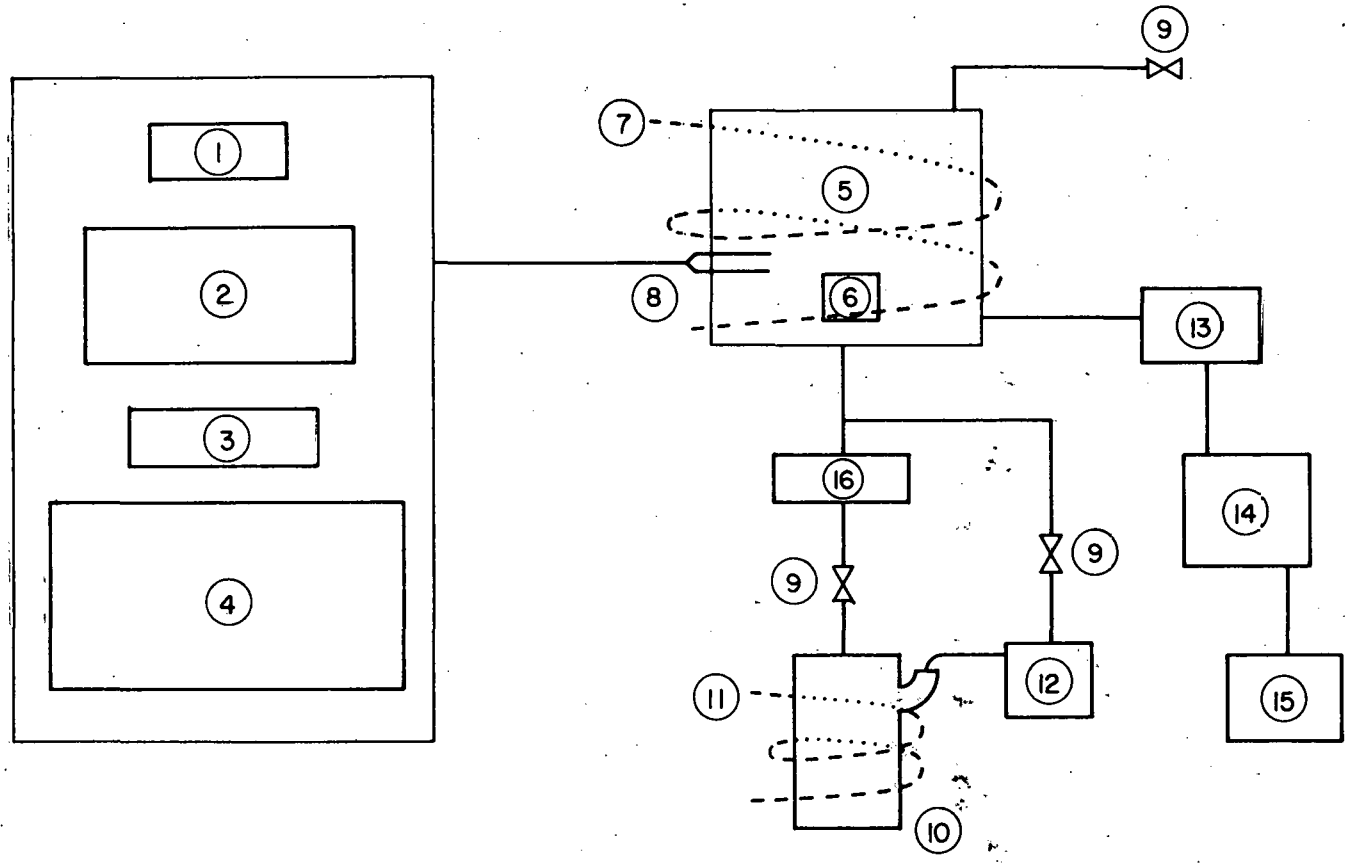

1. PRESSURE GAUGES
2. 'SPEEDOMAX' TEMPERATURE RECORDER
3. 'DATA-TRAC' TEMPERATURE PROGRAMMER
4. VACUUM AND FURNACE CONTROLS
5. 'CENTORR' HI-VAC FURNACE
6. CRUCIBLE
7. FURNACE COOLING JACKET
8. TEMP. & PRESSURE SENSORS
9. PNEUMATIC VALVE
10. 'CVC' DIFFUSION PUMP
11. DIFF. PUMP COOLING JACKET
12. MECHANICAL PUMP
13. QUADRUPOLE PROBE
14. 'UTI' PRECISION GAS ANALYZER
15. 'MFE' TWO-PEN RECORDER
16. LIQ. NITROGEN COLD TRAP

FIGURE 2 DEUTERIUM RELEASE SYSTEM

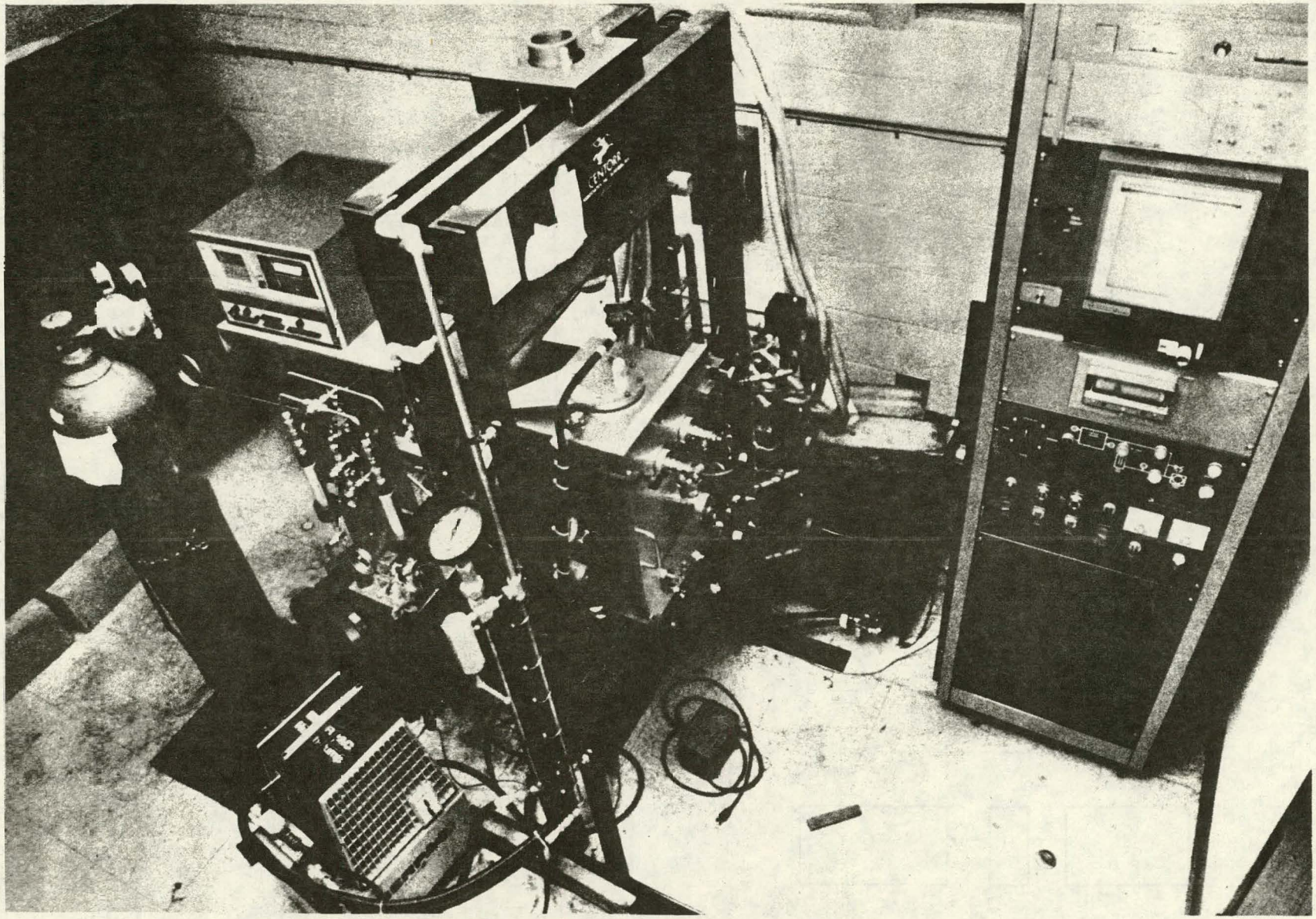

FIGURE 3 PHOTOGRAPH OF DEUTERIUM RELEASE APPARATUS

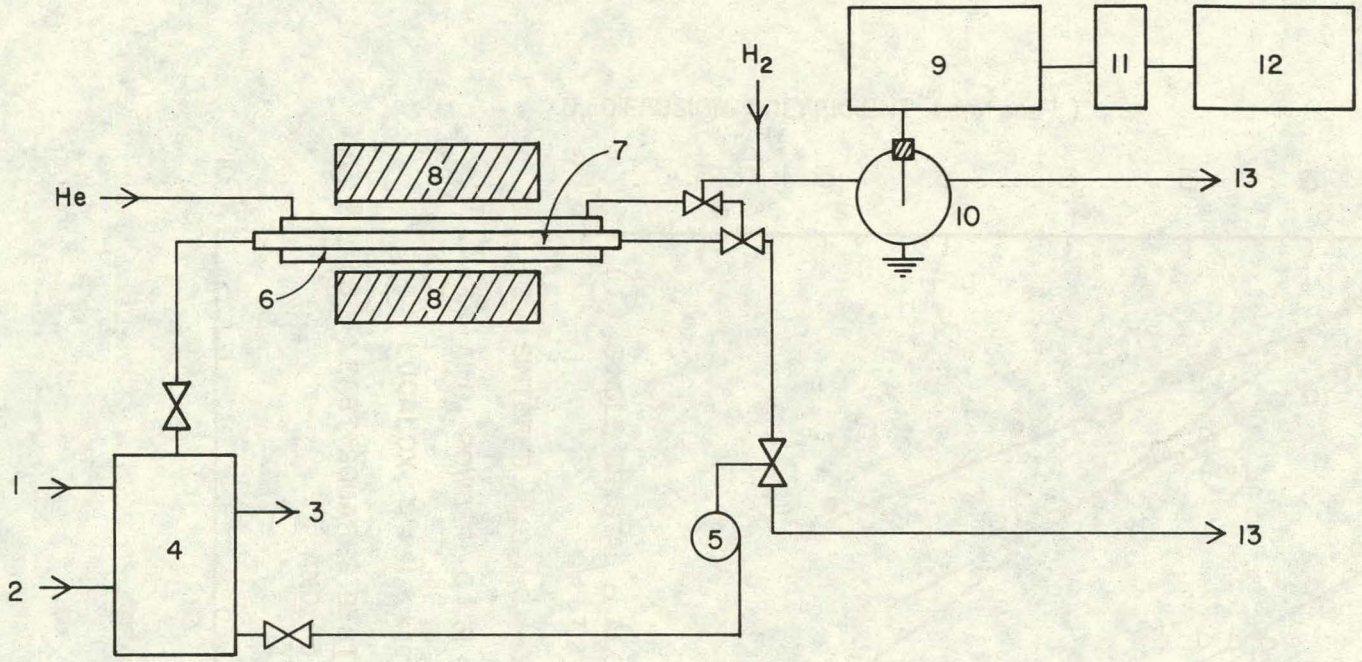

1. He + H_2 FLOW
2. TRITIUM GAS INPUT
3. GRAB SAMPLER
4. CONSTANT VOLUME RESERVOIR
5. MICRO-BELLOWS PUMP
6. HELIUM SWEEP JACKET (Al_2O_3)
7. ALUMINA SAMPLE TUBE
8. FURNACE
9. ELECTROMETER
10. ION CHAMBER
11. ANALOG-TO-FREQUENCY CONVERTER
12. PRINTER
13. VENT TO LAB HOOD

FIGURE 4 SCHEMATIC DRAWING OF PERMEATION LOOP

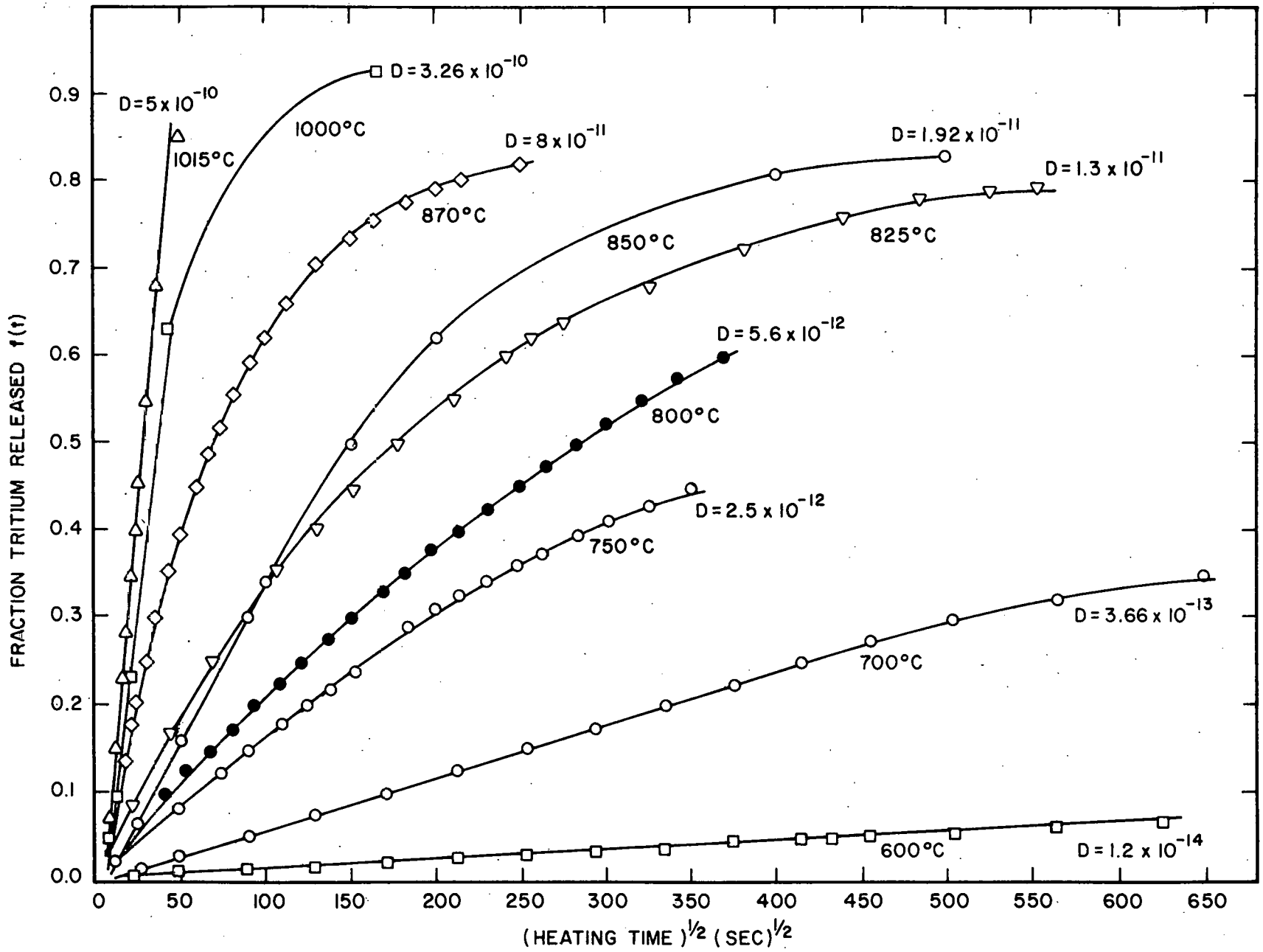

FIGURE 5 RELEASE FRACTION VERSUS $(TIME)^{1/2}$ FOR SINGLE-CRYSTAL α-Al_2O_3 AT DIFFERENT TEMPERATURES

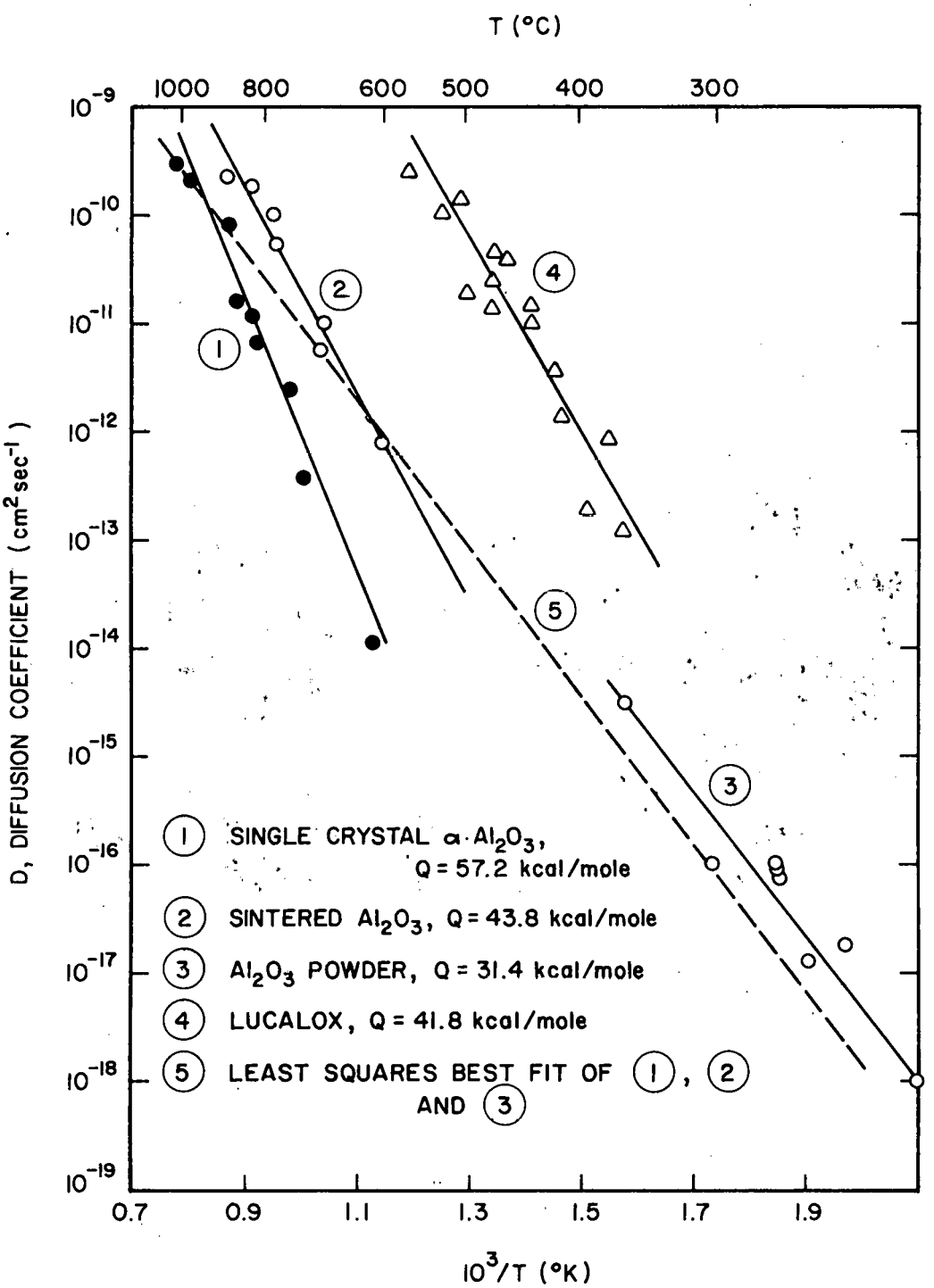

FIGURE 6 MEASURED DIFFUSION COEFFICIENTS FOR TRITIUM DIFFUSION IN α-Al_2O_3

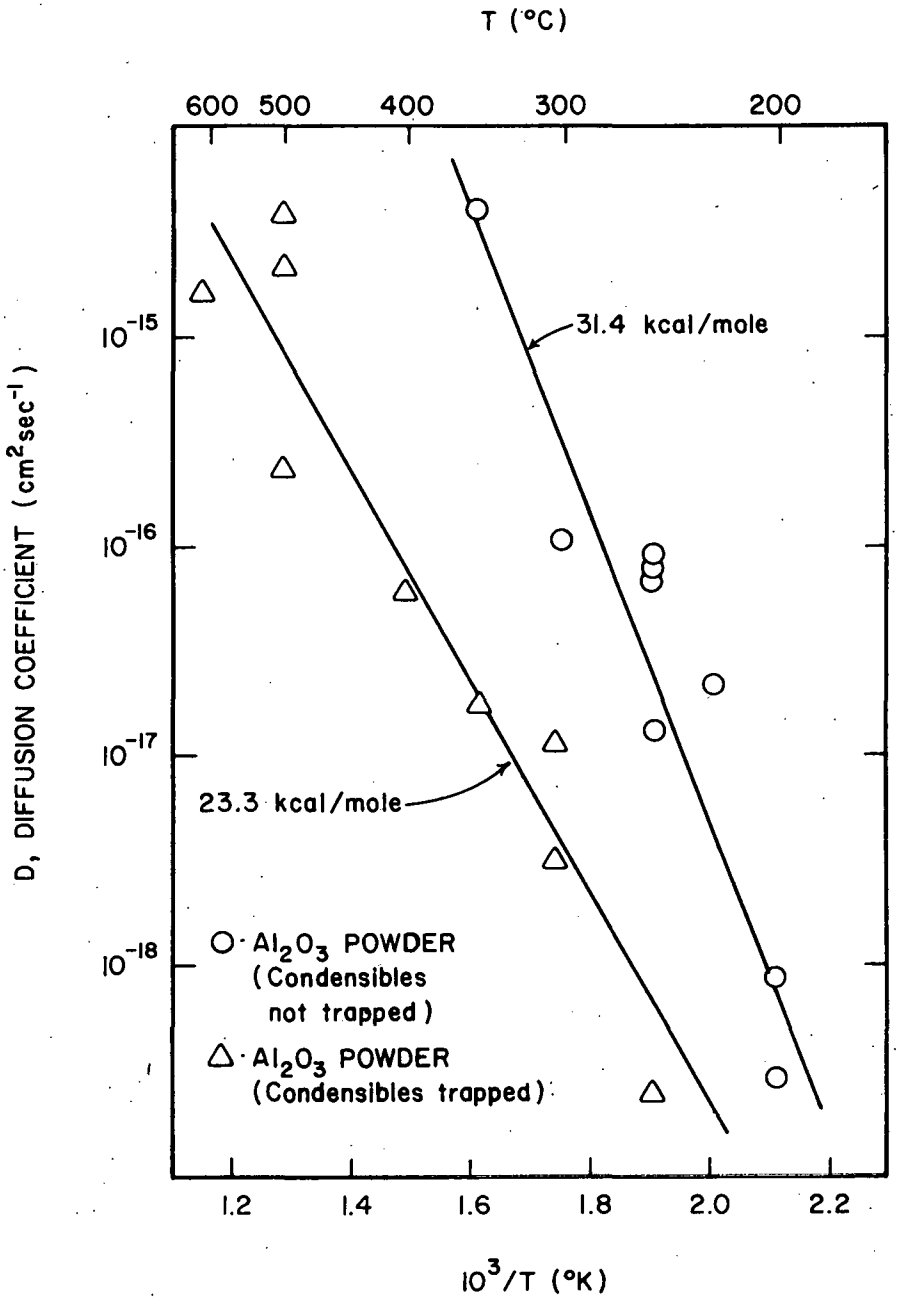

FIGURE 7 EFFECT OF COLD-TRAPPING ON THE APPARENT DIFFUSION COEFFICIENTS FOR Al_2O_3 POWDERS

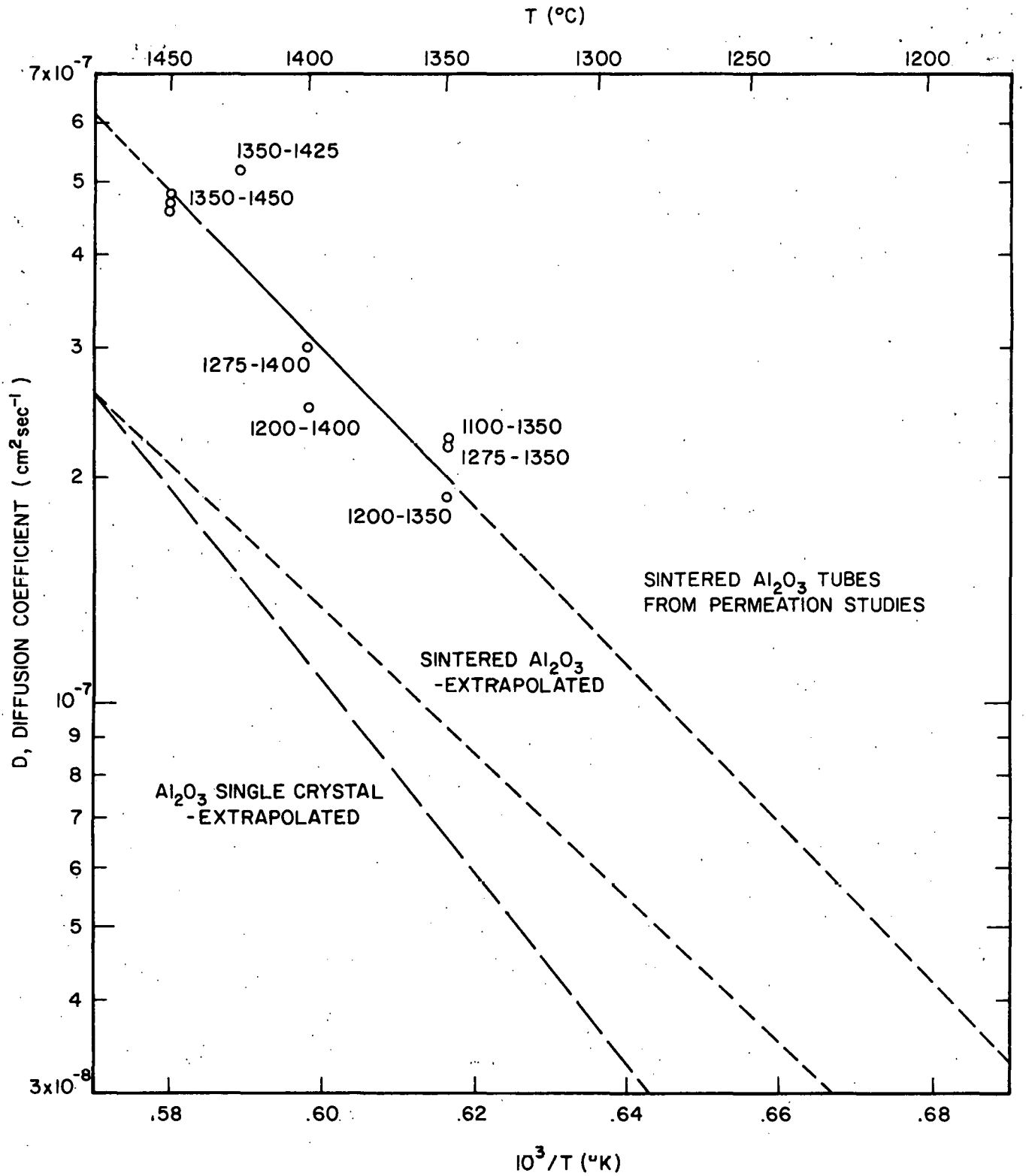

FIGURE 8 COMPARISON OF TRITIUM DIFFUSION COEFFICIENTS IN SINTERED Al_2O_3 TUBES WITH THE VALUES DETERMINED BY RECOIL INJECTION

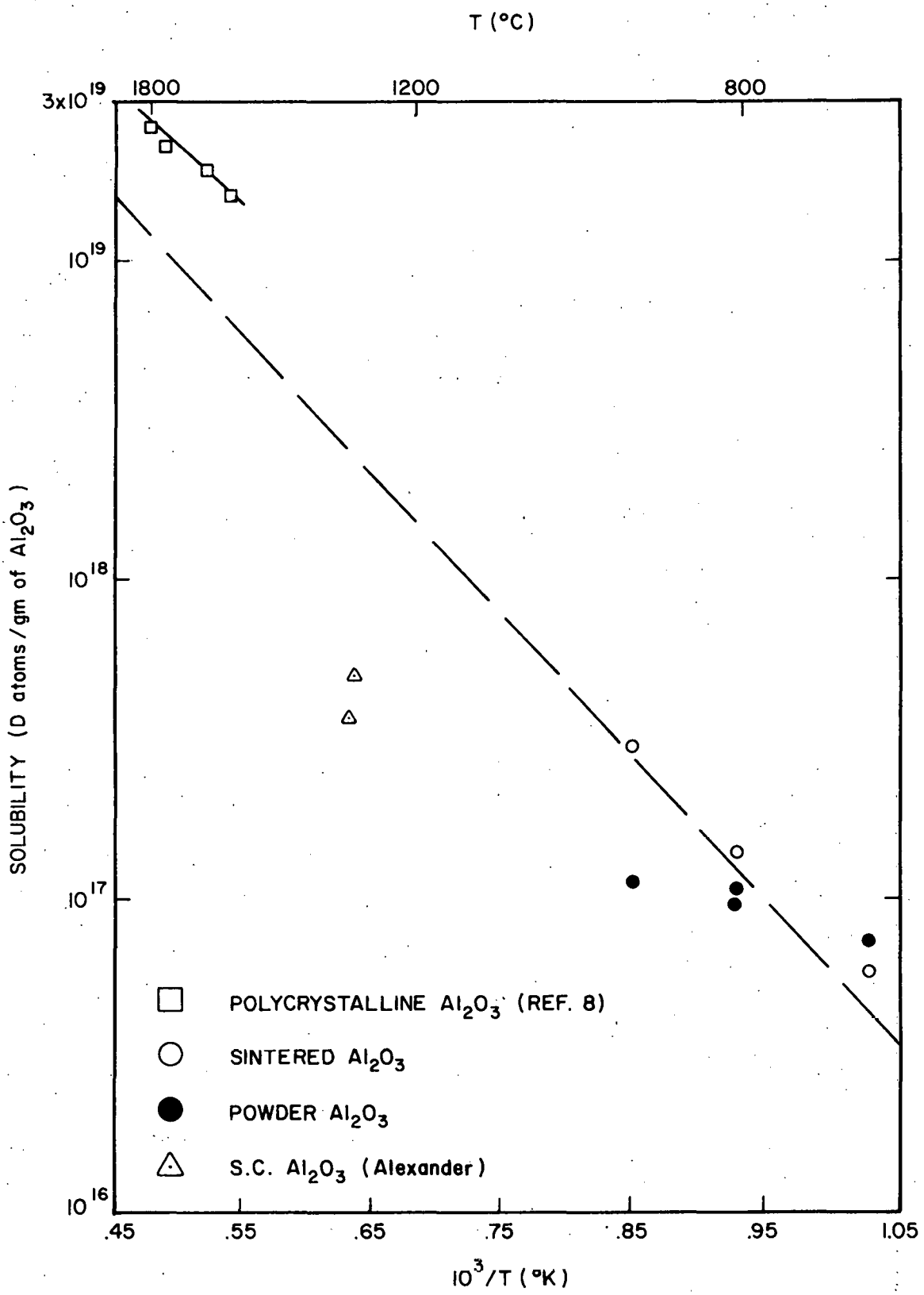

FIGURE 9 HYDROGEN SOLUBILITY IN ALUMINA AT ONE ATMOSPHERE

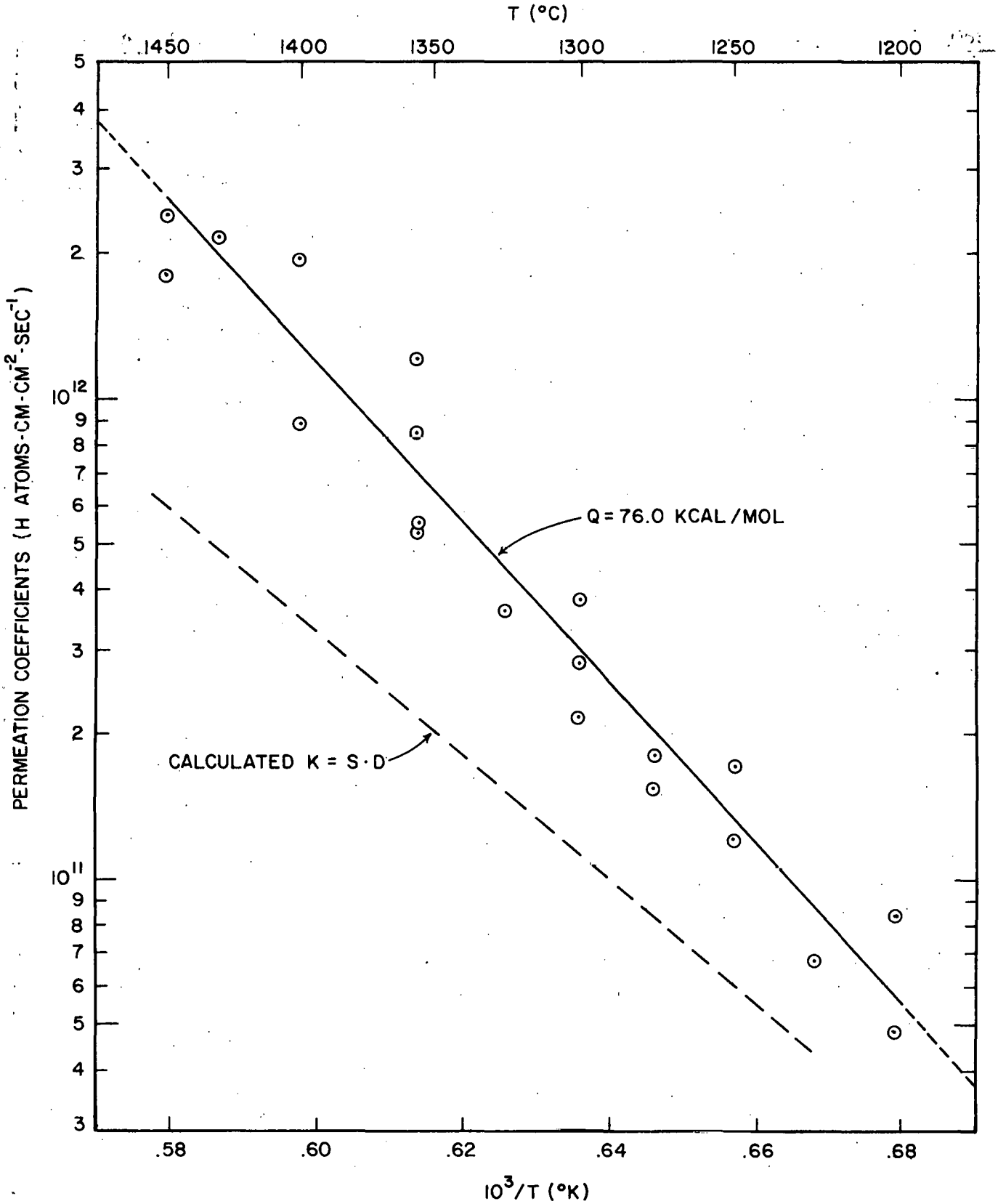

FIGURE 10 MEASURED AND CALCULATED HYDROGEN PERMEATION COEFFICIENTS IN ALUMINUM OXIDE AT ONE ATM

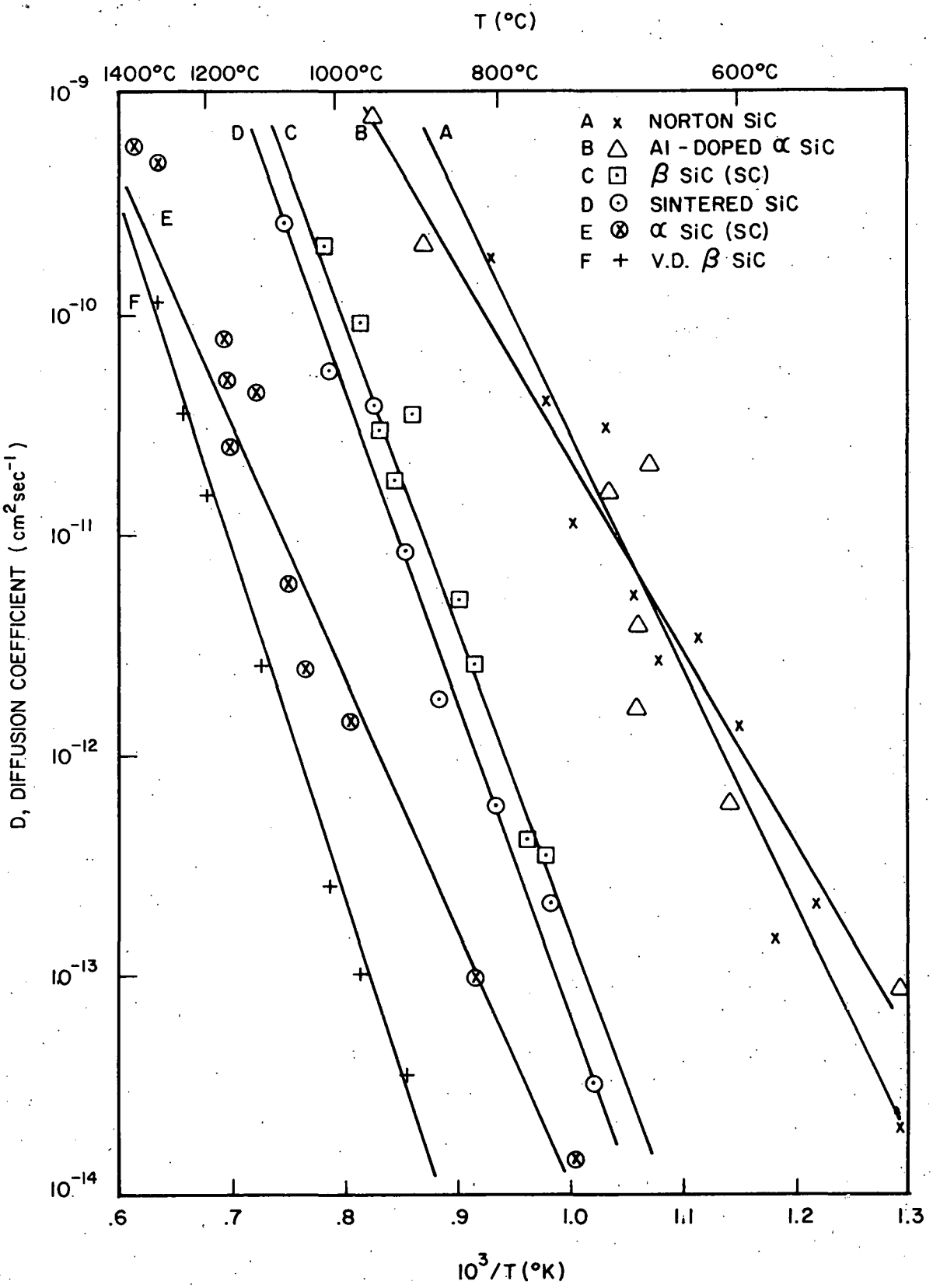

FIGURE 11 MEASURED TRITIUM DIFFUSION COEFFICIENTS IN SiC

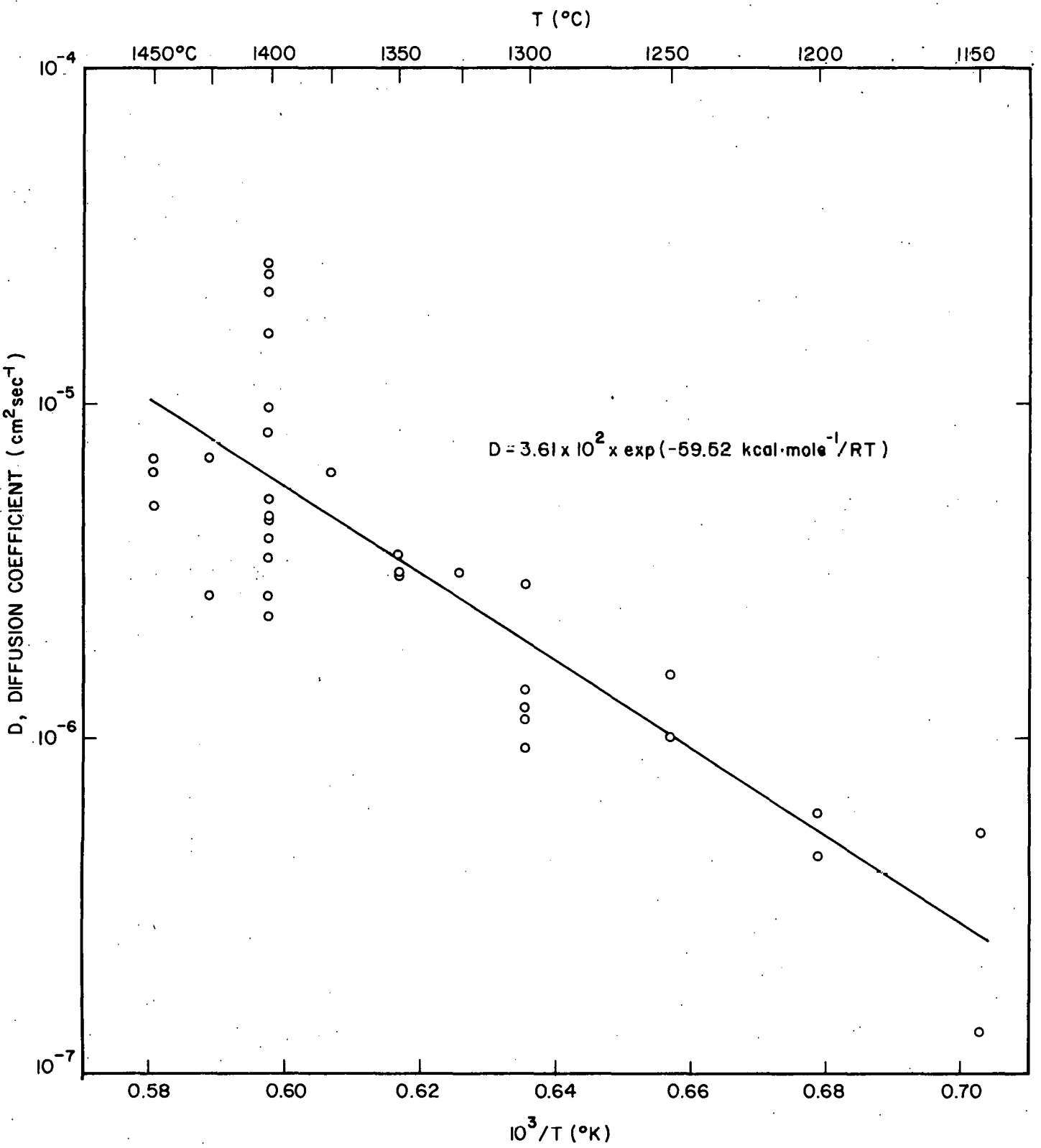

FIGURE 12 HYDROGEN DIFFUSION COEFFICIENTS IN KT-SiC TUBES (VALUES DETERMINED FROM RELEASE KINETICS DURING TEMPERATURE CHANGES)

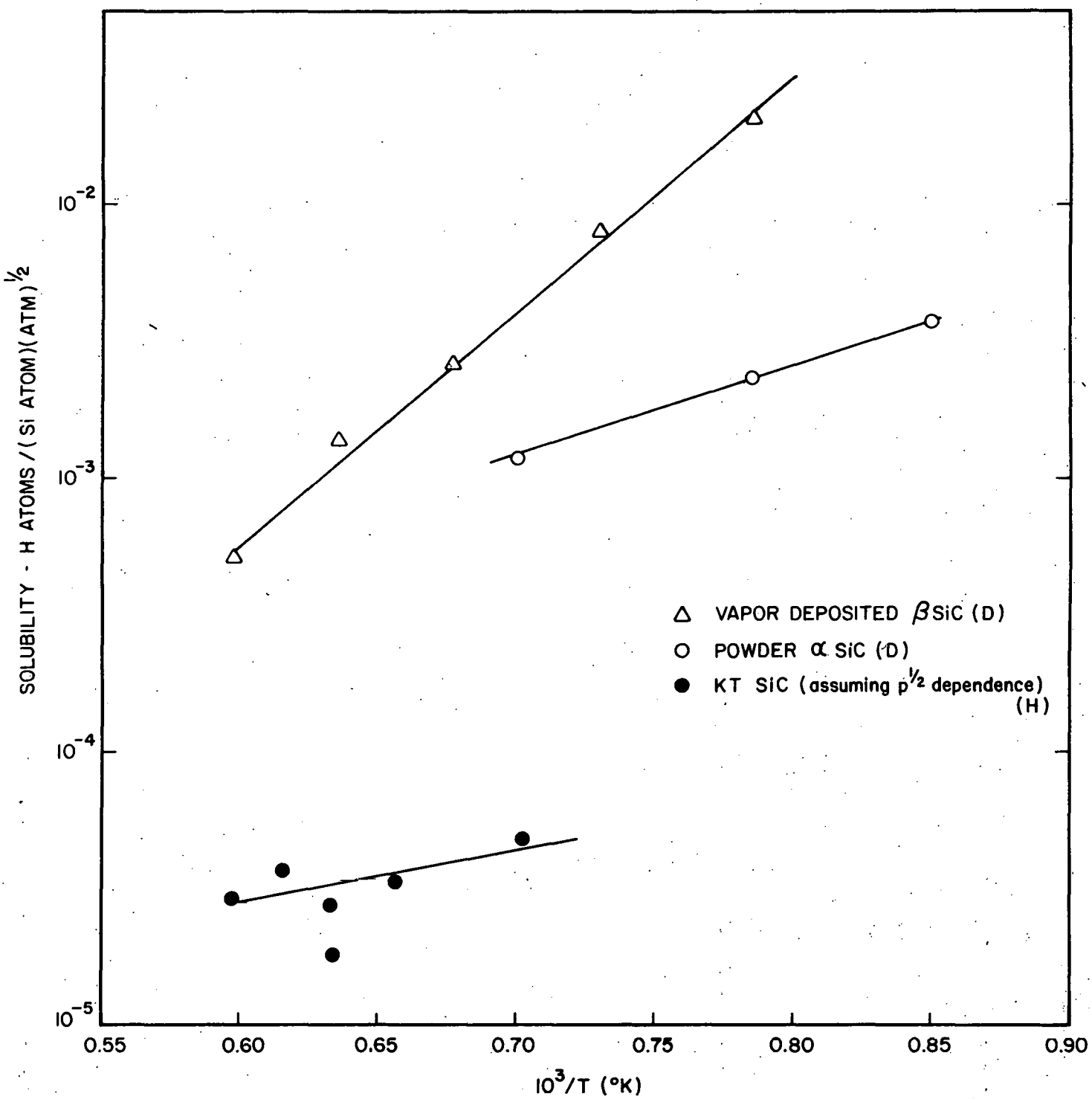

FIGURE 13 HYDROGEN SOLUBILITY IN SiC AT ONE ATMOSPHERE

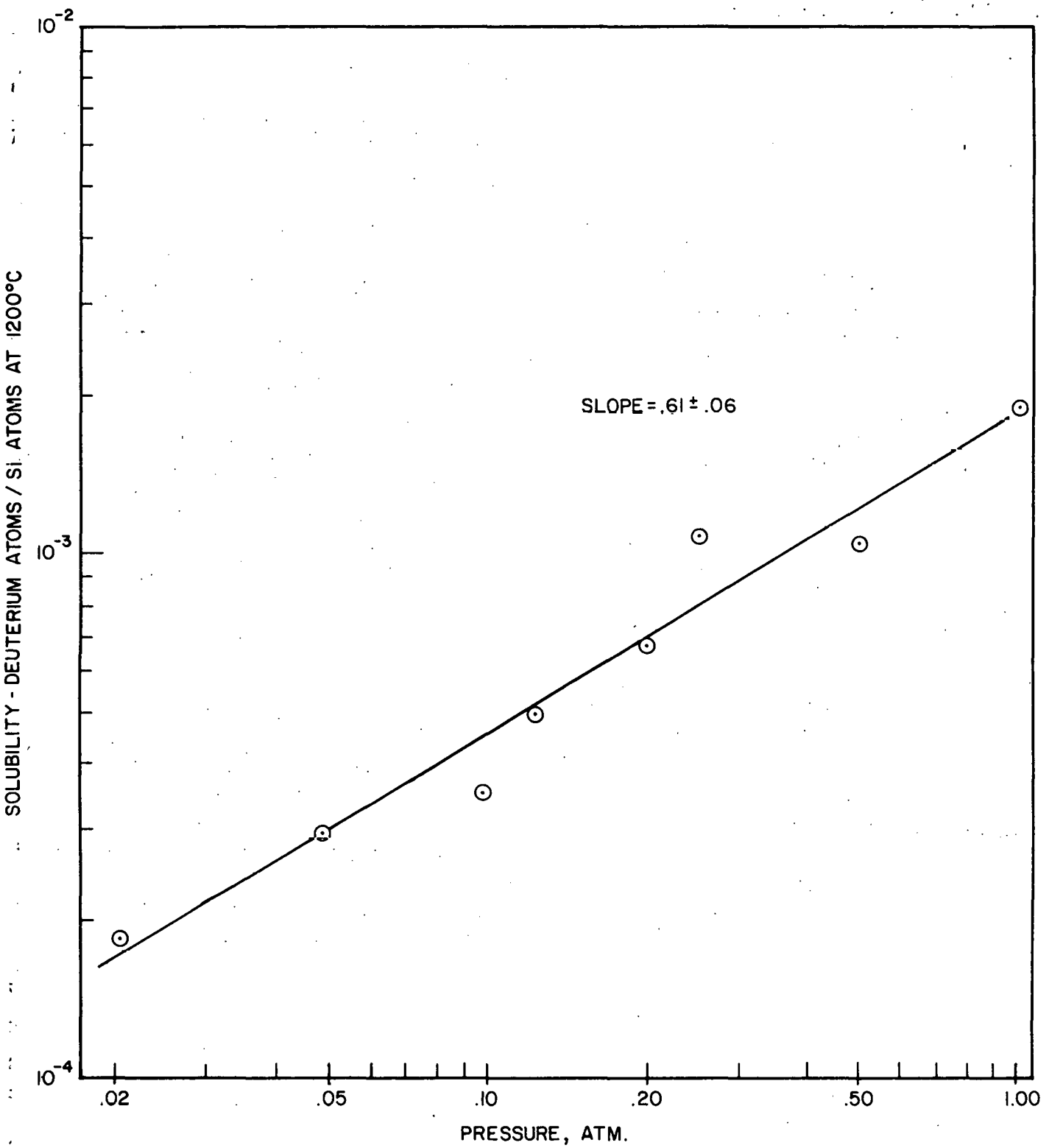

FIGURE 14 DEUTERIUM SOLUBILITY IN VAPOR DEPOSITED β SiC AS A FUNCTION OF DEUTERIUM PRESSURE

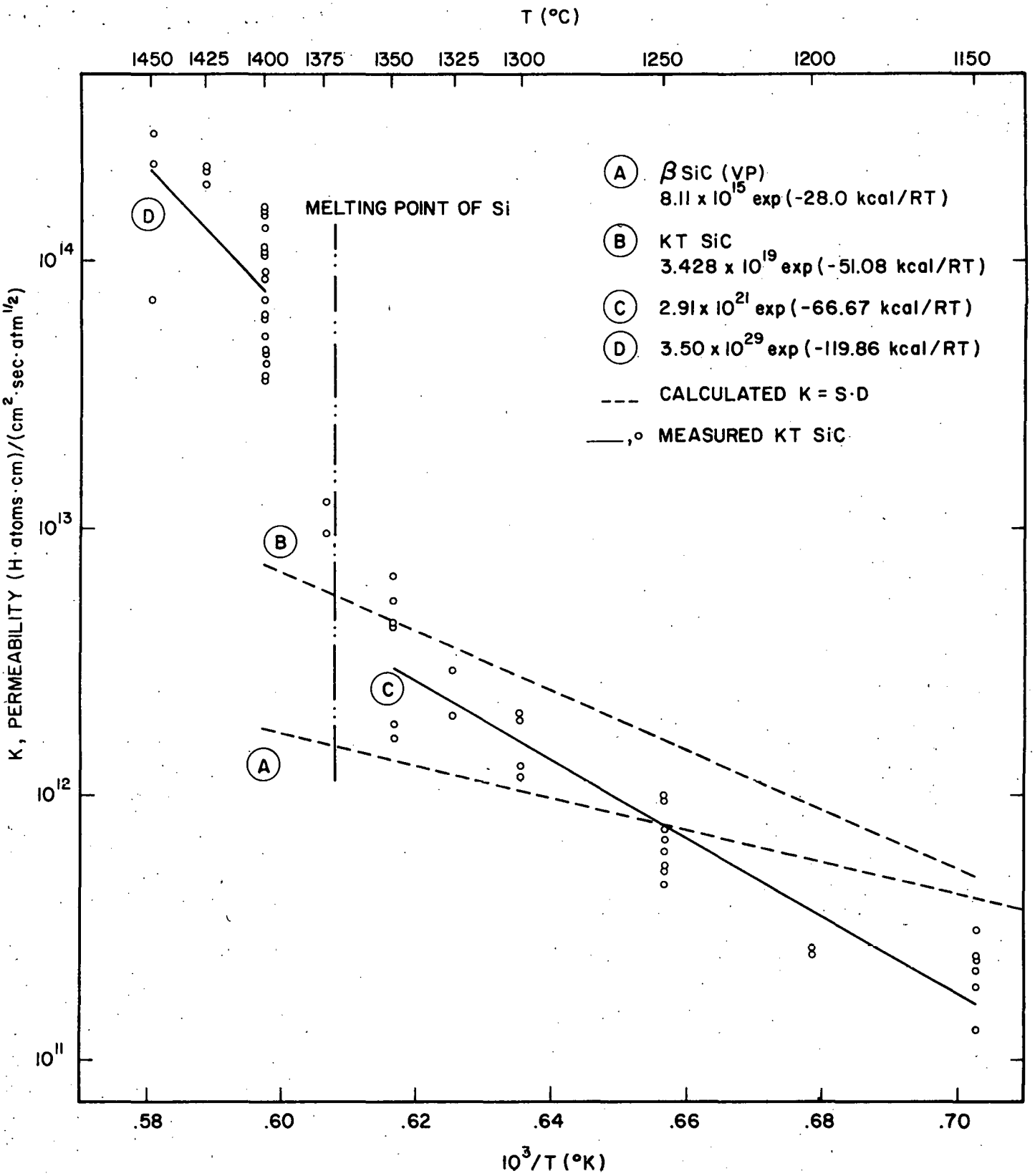

FIGURE 15 MEASURED AND CALCULATED HYDROGEN PERMEABILITY OF SiC

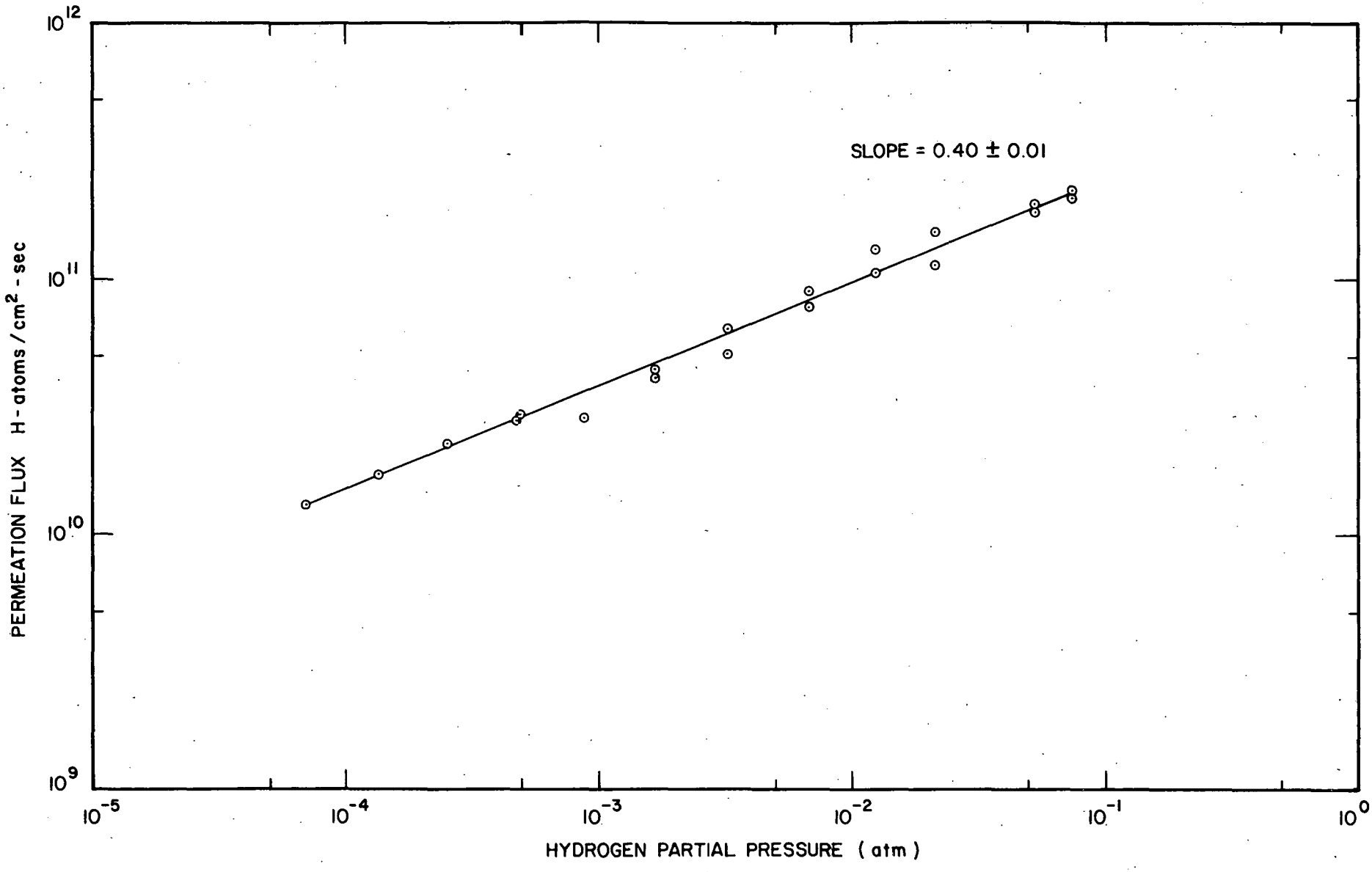

FIGURE 16 PRESSURE DEPENDENCE OF HYDROGEN PERMEATION THROUGH KT·SiC TUBE AT 1250°C

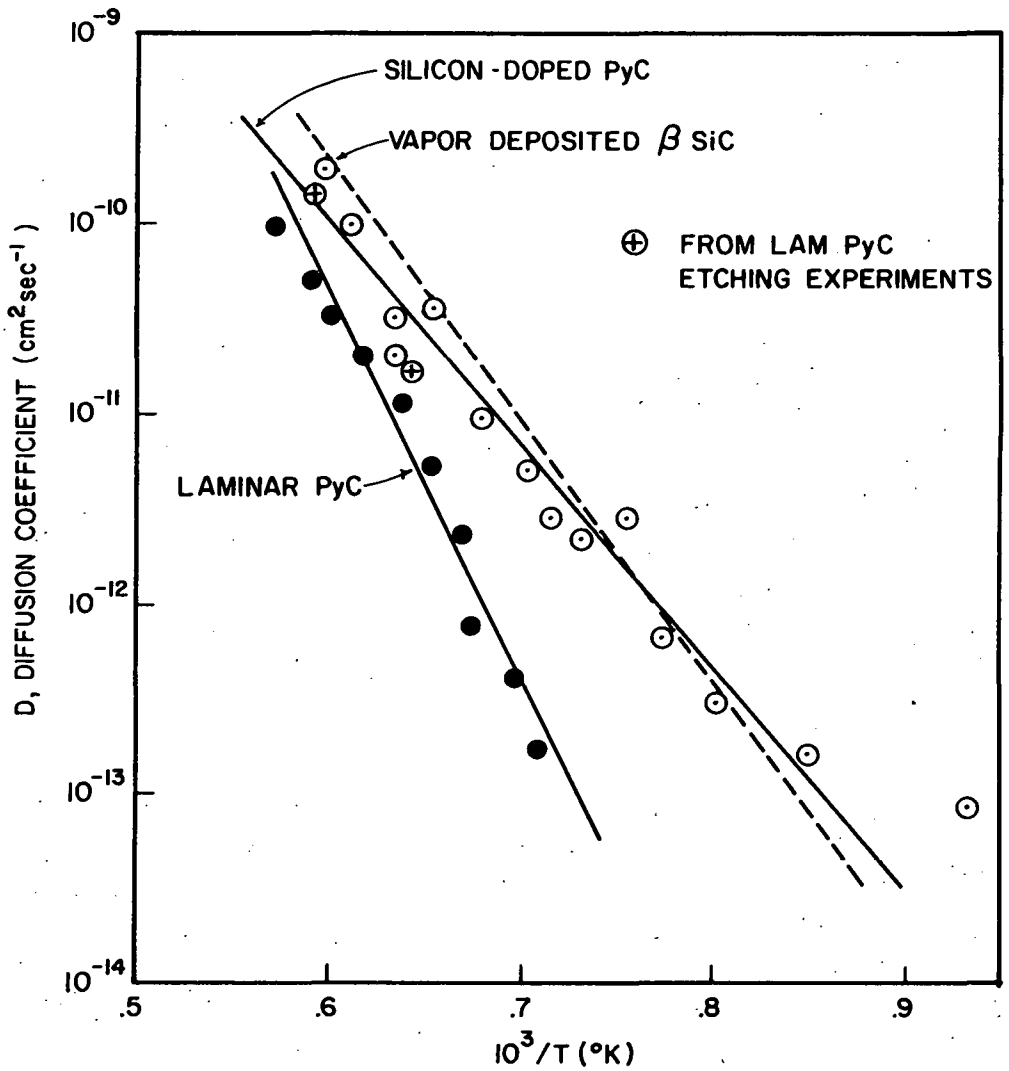

FIGURE 17 COMPARISON OF TRITIUM DIFFUSION COEFFICIENTS IN LAMINAR PYROLYTIC CARBON, SILICON-DOPED PYROLYTIC CARBON AND VAPOR DEPOSITED β-SiC

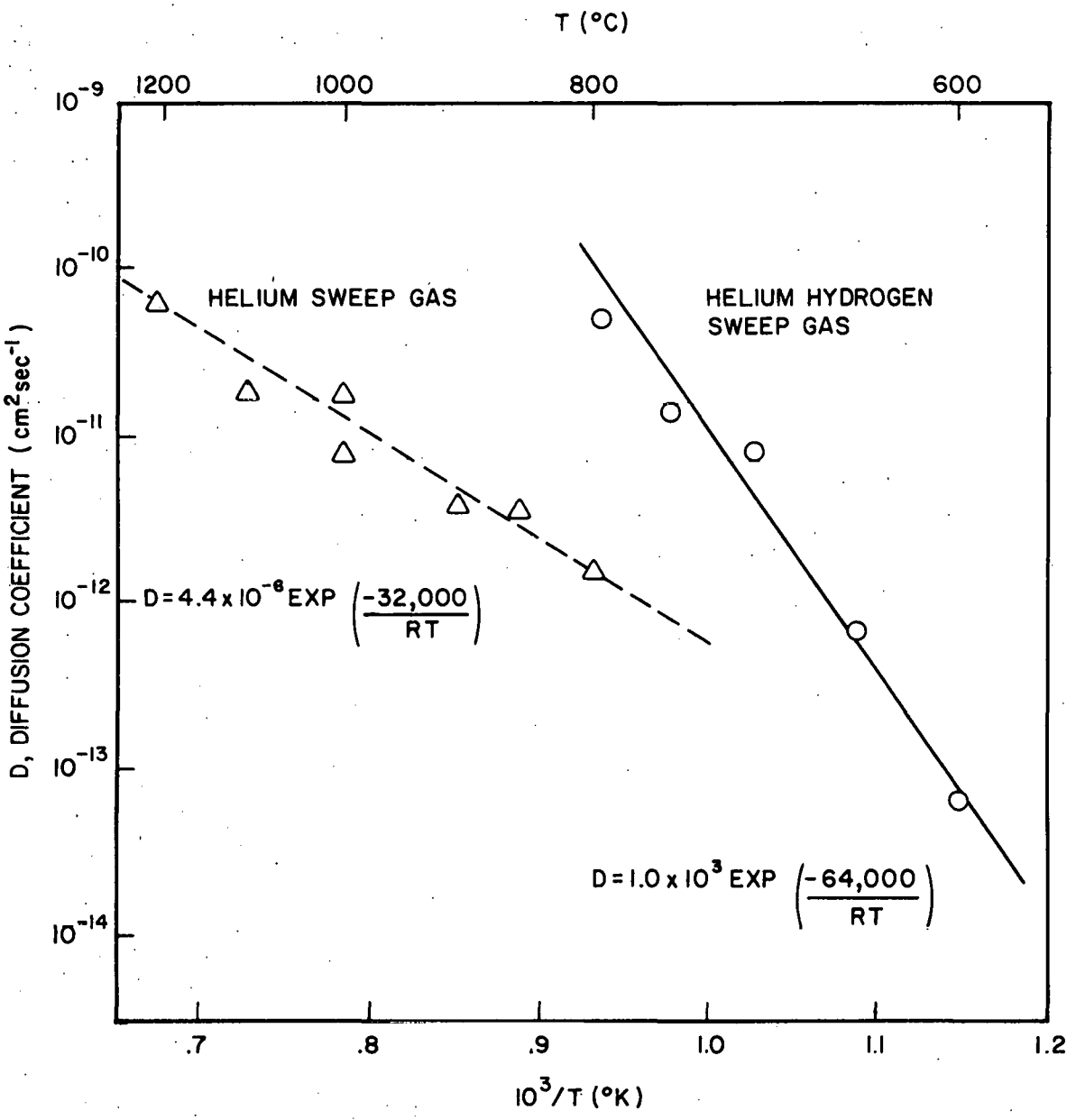

FIGURE 18 ANOMALOUS TRITIUM DIFFUSION RESULTS IN LTI PYROLYTIC CARBON

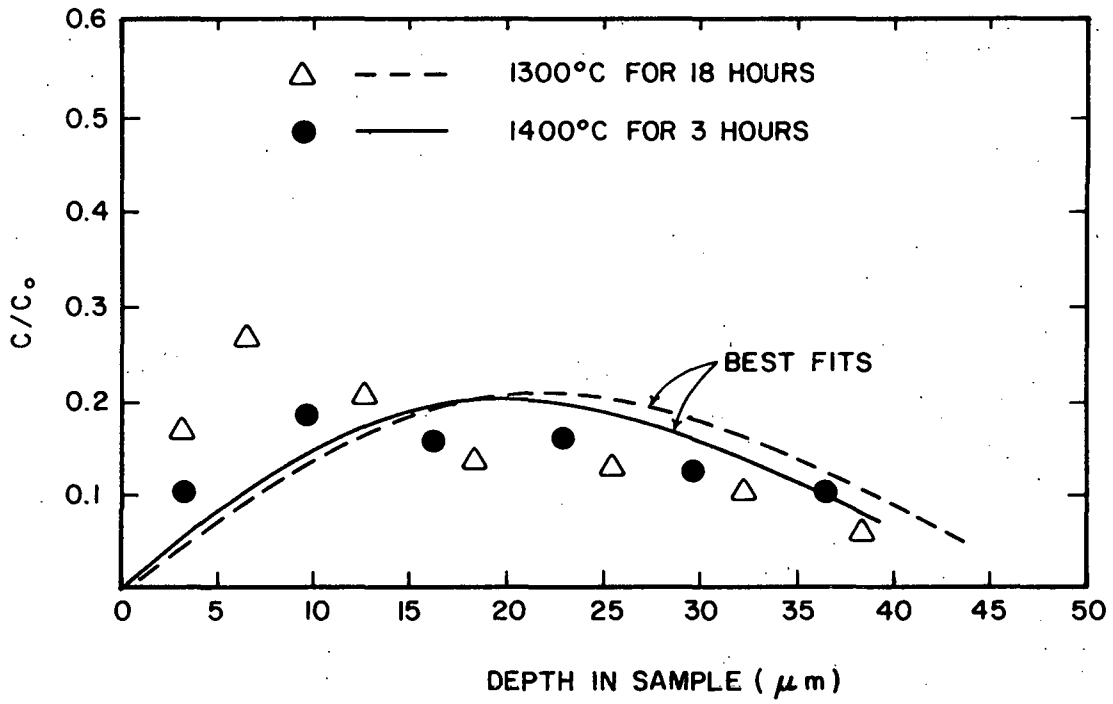

FIGURE 19 TRITIUM CONCENTRATION PROFILE DATA AND CORRESPONDING BEST FIT CURVES IN LAMINAR PYROLYTIC CARBON FOR TWO DIFFERENT ANNEALING CONDITIONS

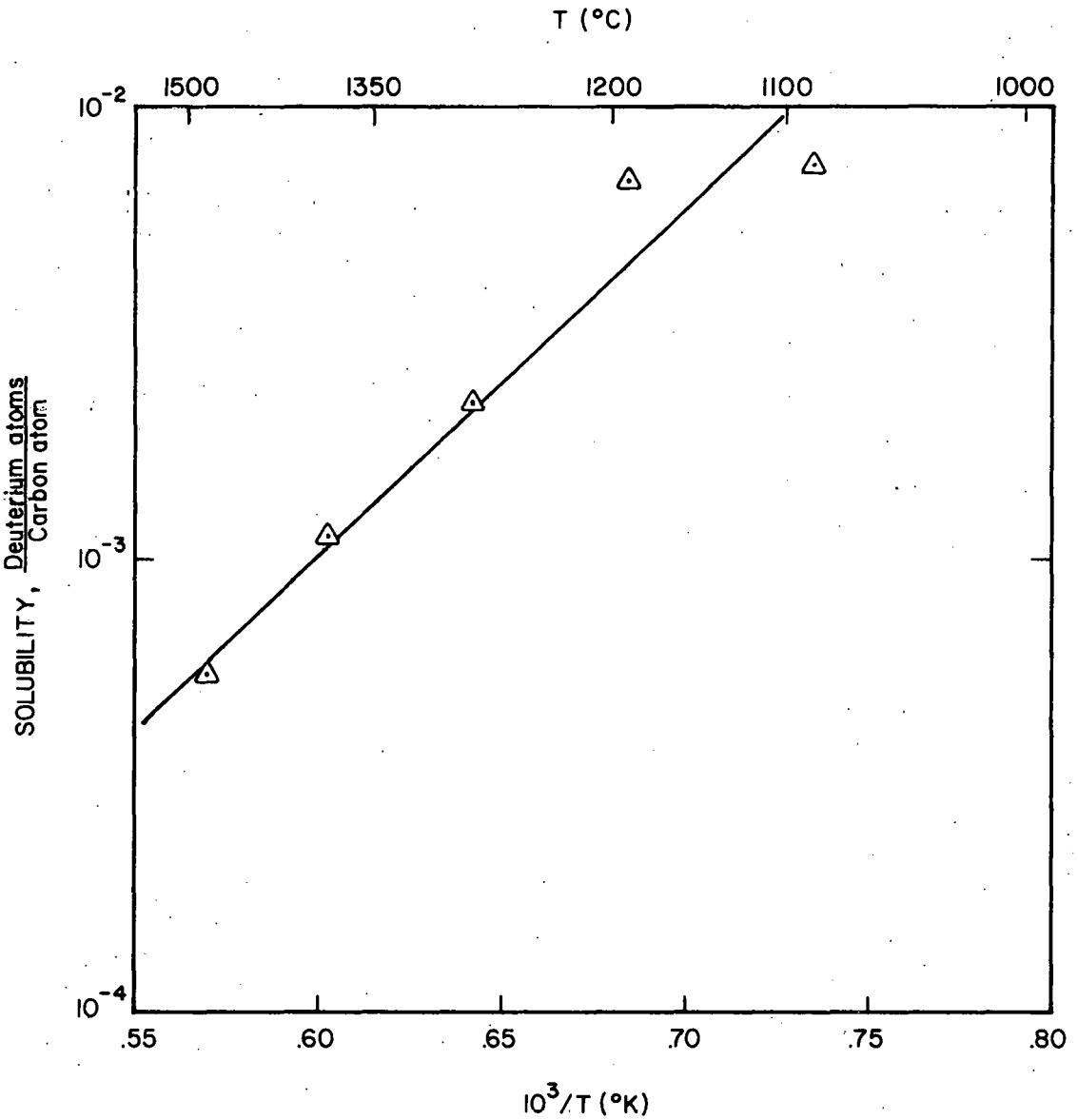

FIGURE 20 DEUTERIUM SOLUBILITY AT ONE ATMOSPHERE IN LAMINAR PYROLYTIC CARBON AS A FUNCTION OF TEMPERATURE

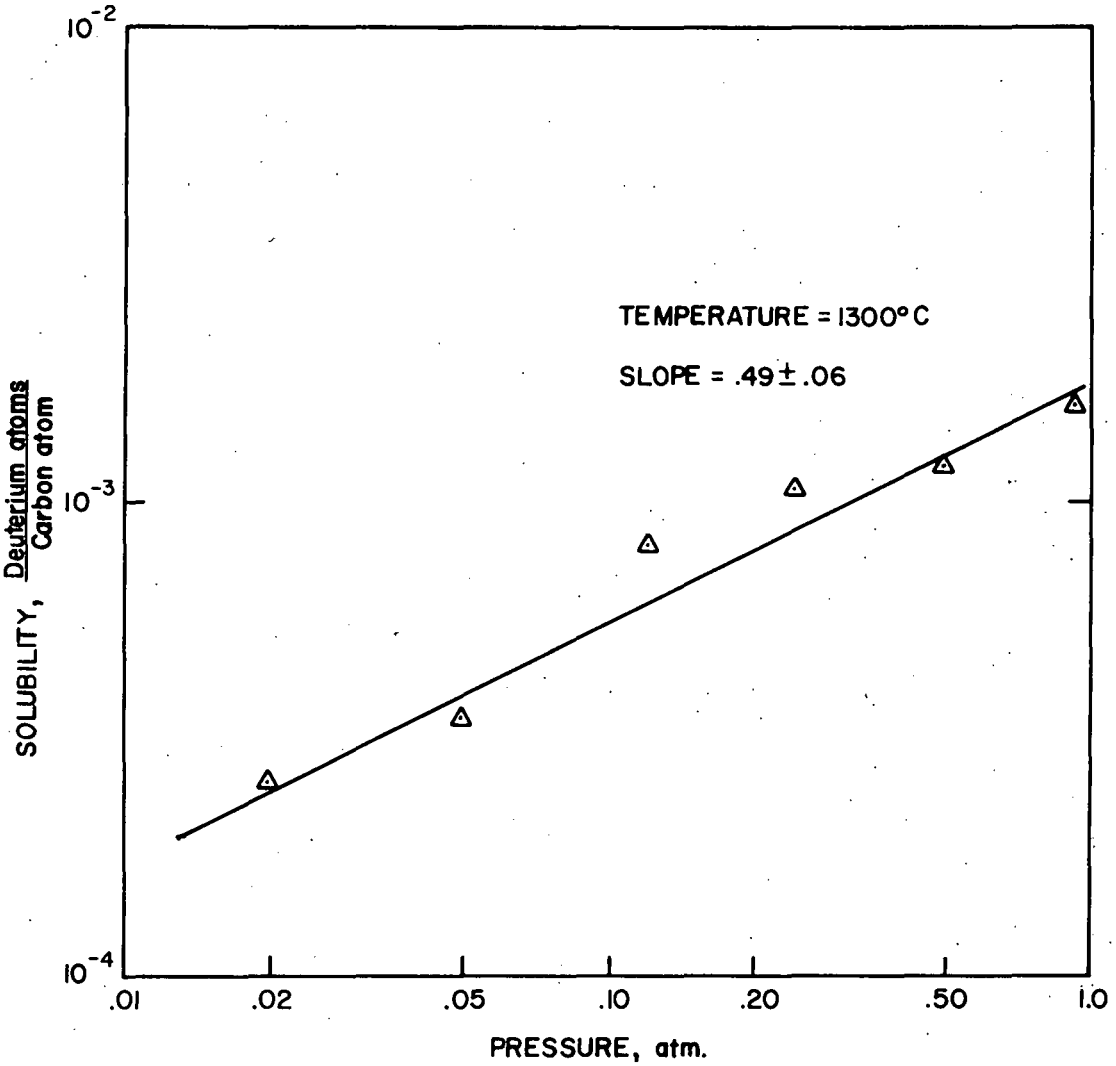

FIGURE 21 DEUTERIUM SOLUBILITY AT 1300° C IN LAMINAR PYROLYTIC CARBON AS A FUNCTION OF PRESSURE

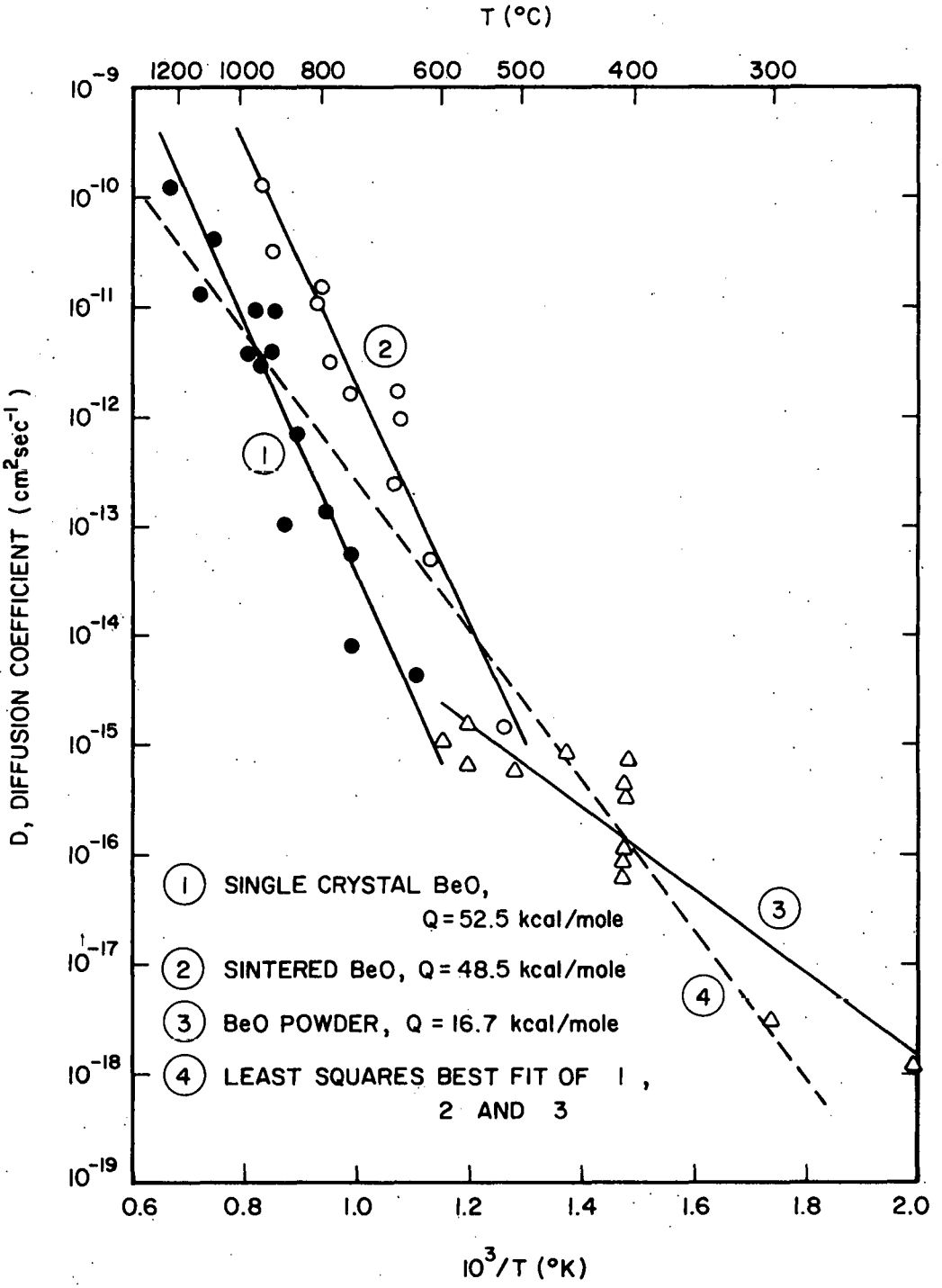

FIGURE 22 MEASURED TRITIUM DIFFUSION COEFFICIENTS IN BeO

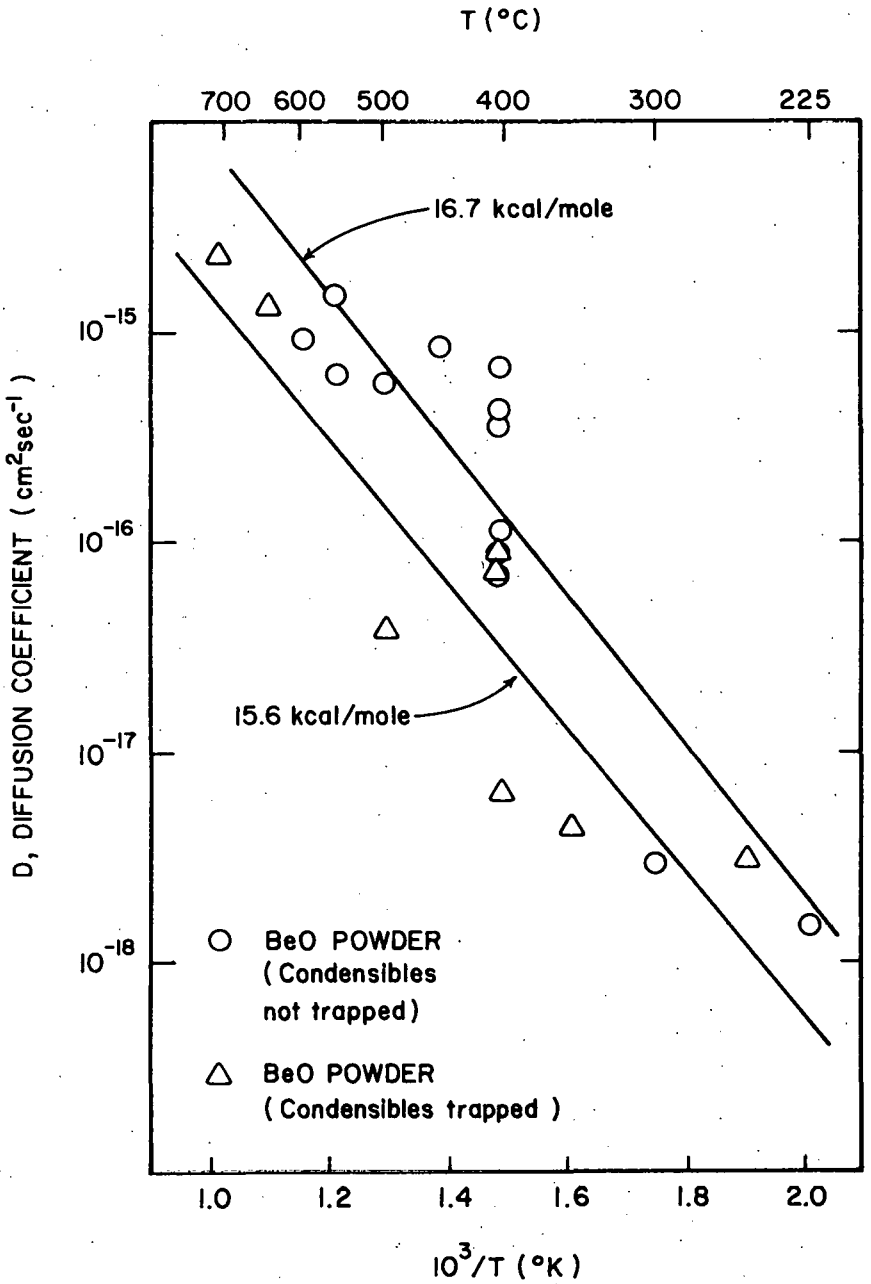

FIGURE 23 EFFECT OF COLD-TRAPPING ON THE APPARENT DIFFUSION COEFFICIENTS FOR BeO POWDERS

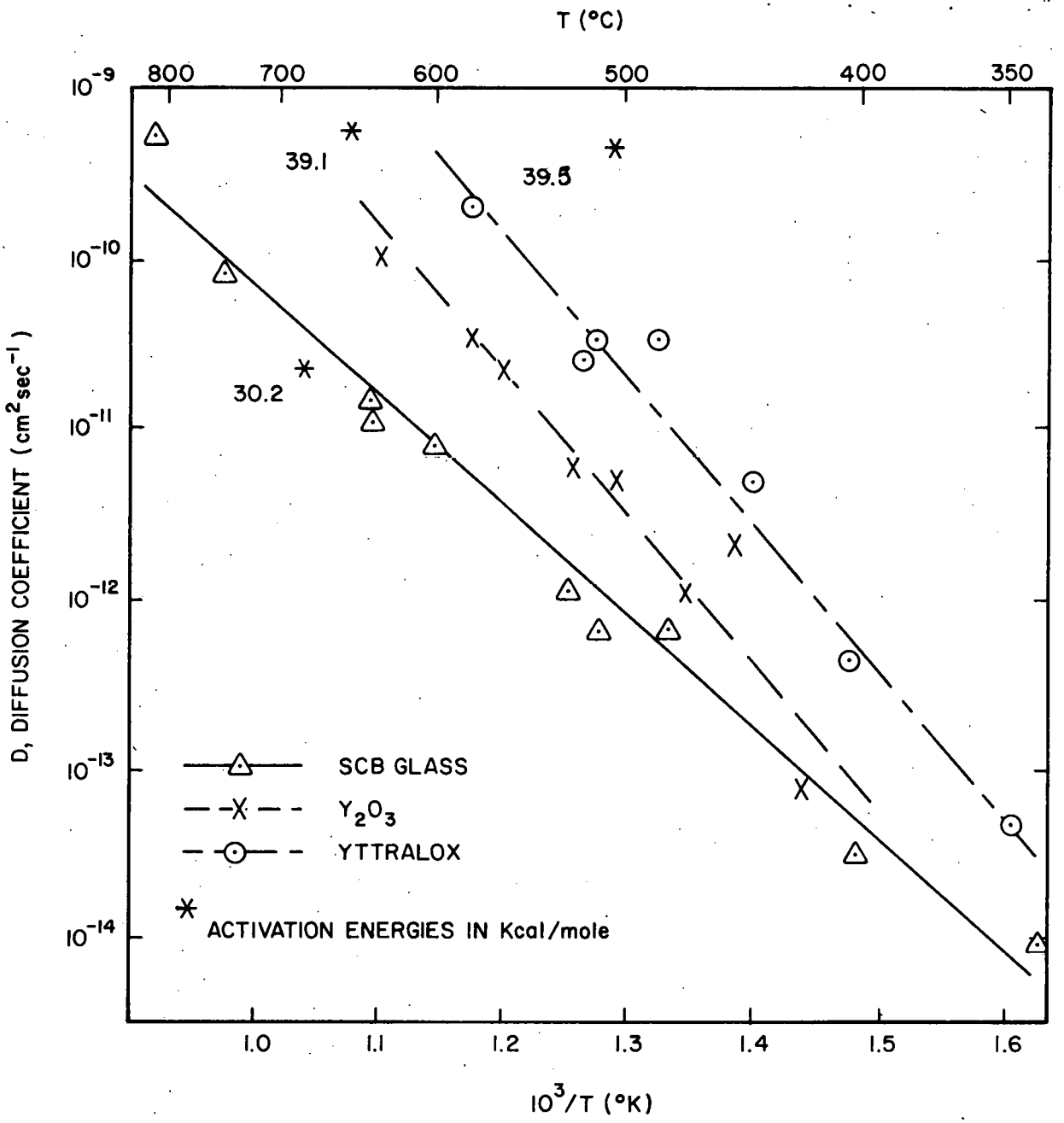

FIGURE 24 ARRHENIUS PLOT FOR TRITIUM DIFFUSION IN SCB GLASS, YTTRIA AND YTTRALOX

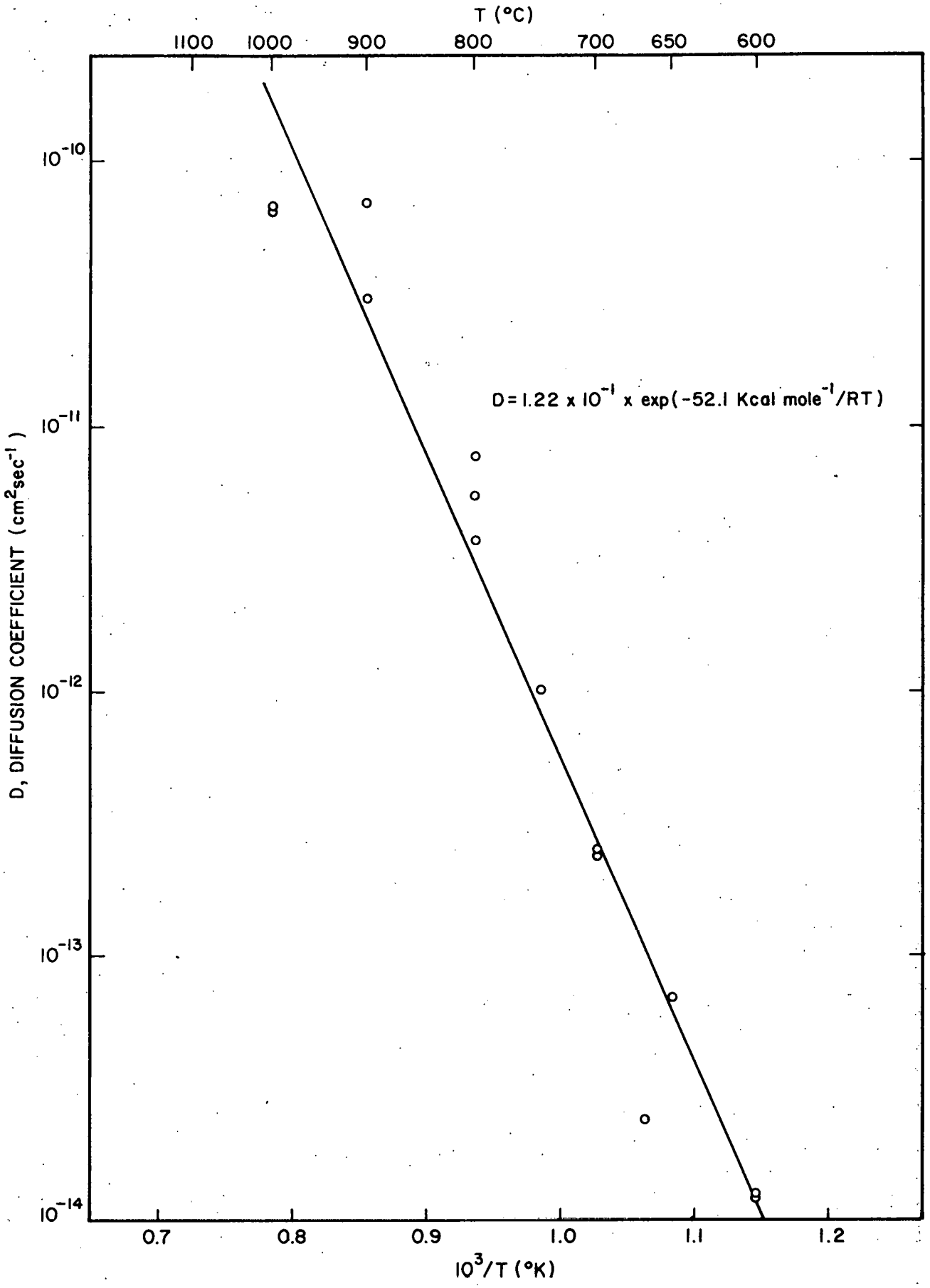

FIGURE 25 MEASURED DIFFUSION COEFFICIENTS IN SINTERED Si_3N_4

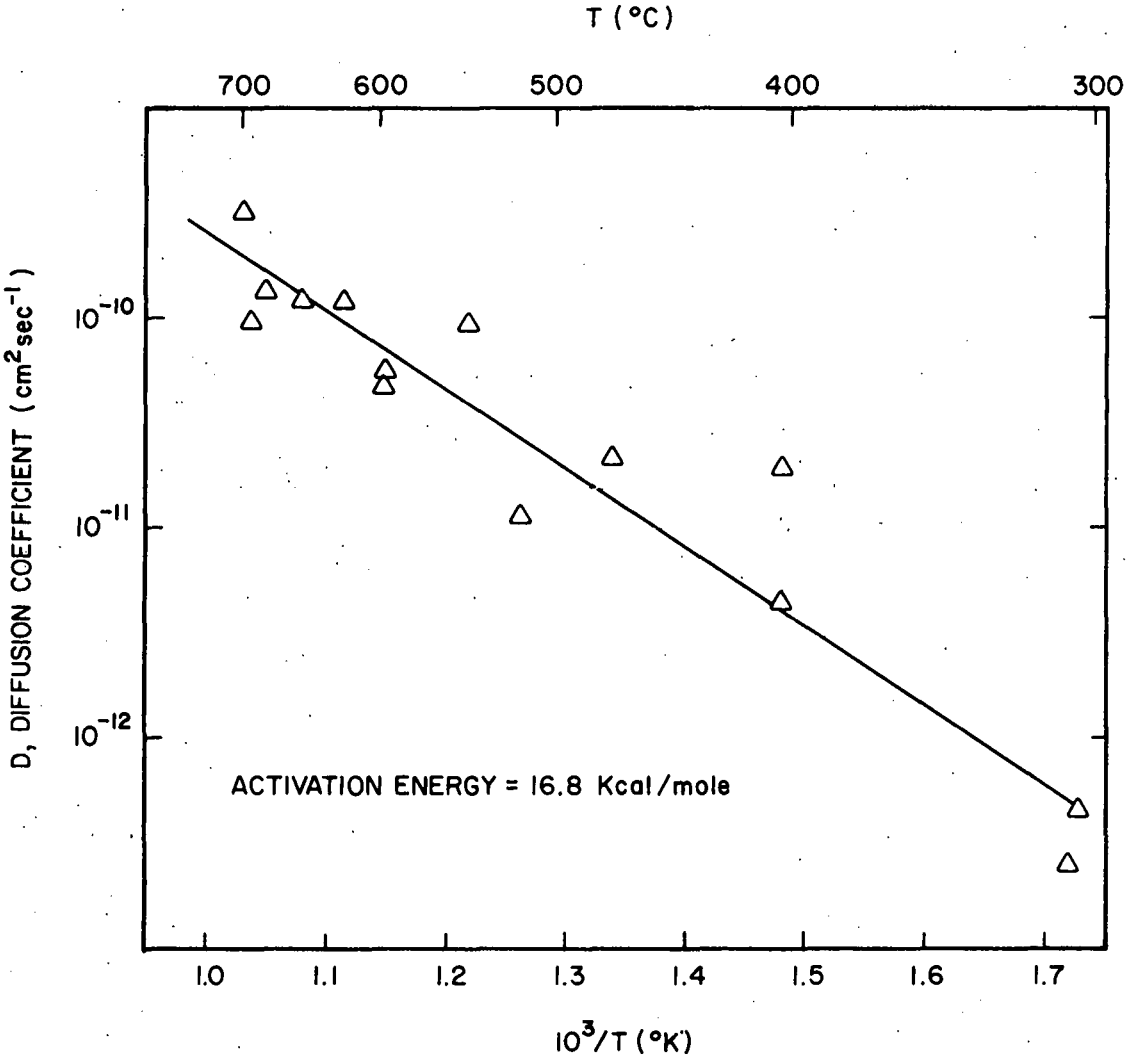

FIGURE 26 MEASURED TRITIUM DIFFUSION COEFFICIENTS IN BORON CARBIDE (B_4C)

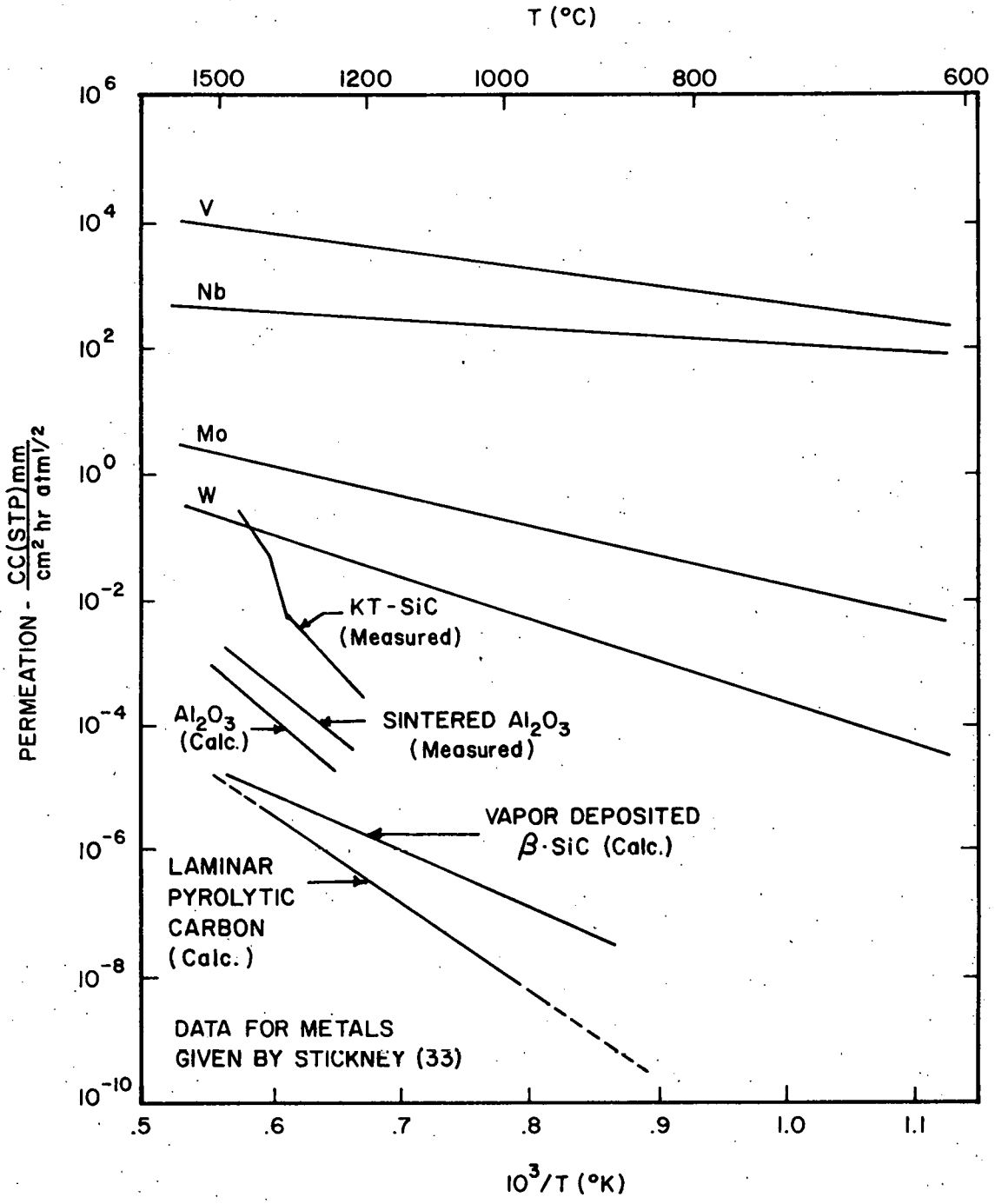

FIGURE 27 COMPARISON OF TRITIUM PERMEATION IN Al_2O_3, SiC AND PyC TO HYDROGEN PERMEATION IN REFRACTORY METALS

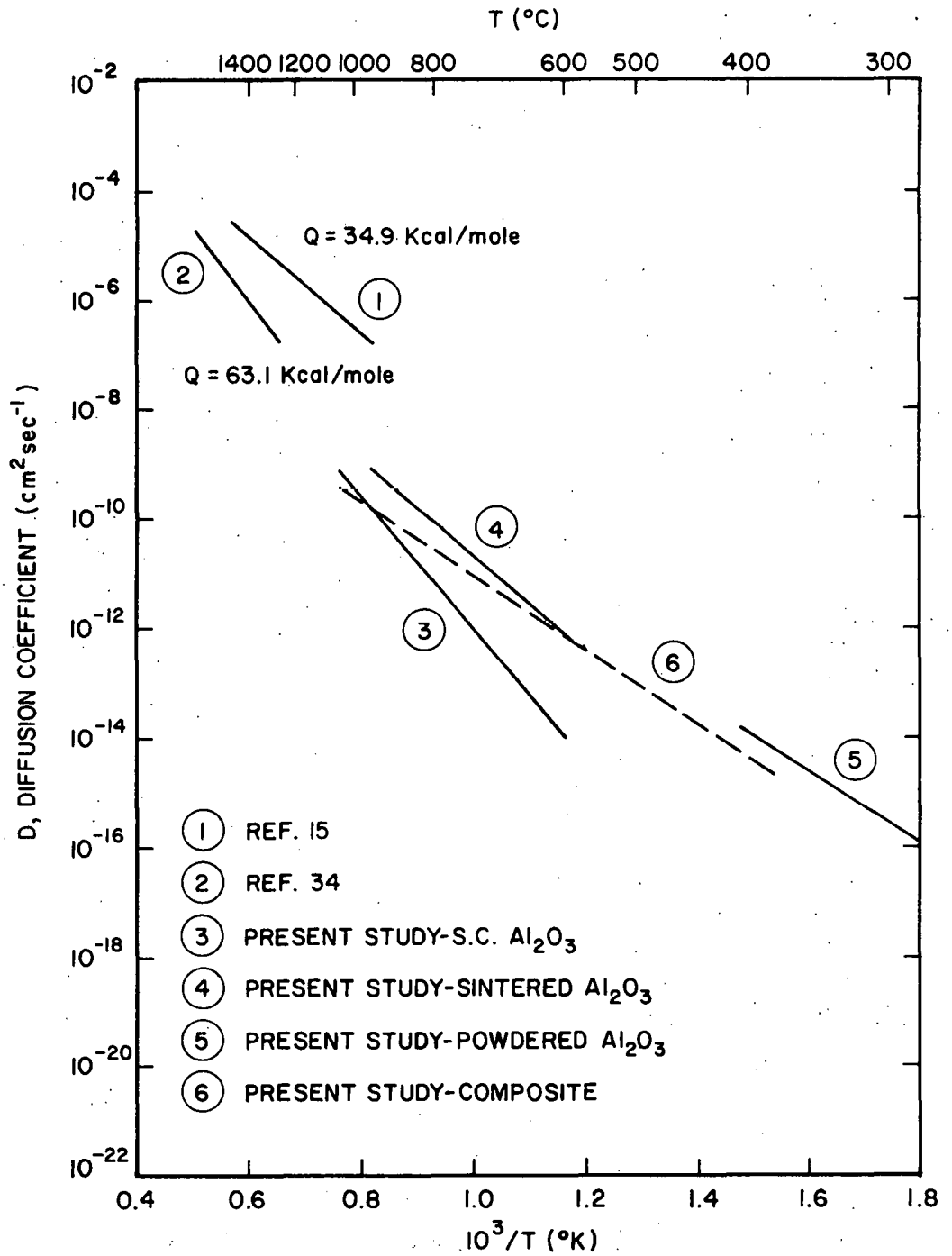

FIGURE 28 A COMPARISON OF REPORTED DIFFUSION COEFFICIENTS FOR Al_2O_3

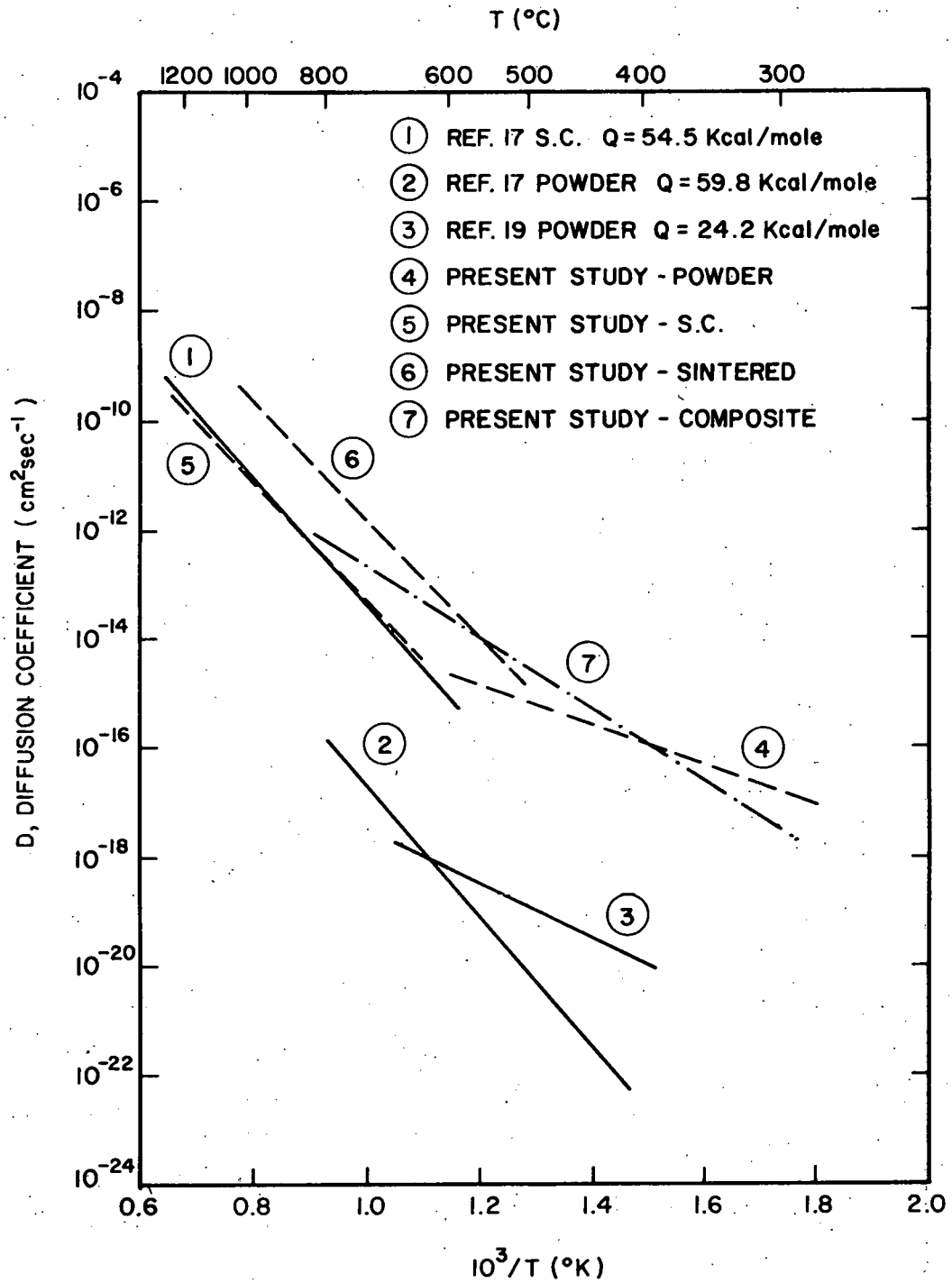

FIGURE 29 A COMPARISON OF REPORTED DIFFUSION COEFFICIENTS FOR BeO